AEI–2014–053
DAMTP–2014–59

Towards one-loop SYM amplitudes from the pure spinor BRST cohomology

Carlos R. Mafra[†] and Oliver Schlotterer[‡]

[†] *DAMTP, University of Cambridge*
Wilberforce Road, Cambridge, CB3 0WA, UK

[‡] *Max–Planck–Institut für Gravitationsphysik*
Albert–Einstein–Institut, 14476 Potsdam, Germany

In this paper, we outline a method to compute supersymmetric one-loop integrands in ten-dimensional SYM theory. It relies on the constructive interplay between their cubic-graph organization and BRST invariance of the underlying pure spinor superstring description. The five- and six-point amplitudes are presented in a manifestly local form where the kinematic dependence is furnished by BRST-covariant expressions in pure spinor superspace. At five points, the local kinematic numerators are shown to satisfy the BCJ duality between color and kinematics leading to supergravity amplitudes as a byproduct. At six points, the sources of the hexagon anomaly are identified in superspace as systematic obstructions to BRST invariance. Our results are expected to reproduce any integrated SYM amplitude in dimensions $D < 8$.

October 2014

[†] email: c.r.mafra@damtp.cam.ac.uk

[‡] email: olivers@aei.mpg.de

Contents

1. Introduction

Recent developments have shown that scattering amplitudes take a much simpler form than the multitude of Feynman diagrams would seem to suggest [1]. In a variety of theories and spacetime dimensions, the laborious computations based on textbook methods were successfully sidestepped by new approaches to determine amplitudes from first principles manifesting their hidden simplicity. Along these lines, this work describes a method to obtain the integrands of one-loop amplitudes in ten-dimensional $\mathcal{N} = 1$ super-Yang–Mills theory (SYM) [2] on the basis of two fundamental principles: locality and BRST symmetry.

Locality refers to the expansion of amplitudes in terms of cubic graphs whose propagators encode the structure of poles and branch cuts in the scattering data [3]. BRST invariance is embedded into pure spinor superspace where it guarantees supersymmetry and gauge invariance as originally described in the context of the pure spinor superstring[1] [7]. This underpins the observation of Howe [8] that pure spinor variables simplify the description of ten-dimensional $\mathcal{N} = 1$ SYM.

In the subsequent, we will explain how to combine locality and BRST invariance to a constructive and intuitive prescription to assemble one-loop integrands of SYM from their cubic-graph expansion. The long-term goal of this approach is to find a general and intuitive mapping from cubic graphs at any loop order to superfields such as the objects V_{12} and $T_{3,4,56}$ as seen on the right. The tree-level mappings have already been worked out in [9,10] and the main result of this paper is a one-loop implementation of this dictionary. Using this method we obtain a local form of the five- and six-point one-loop integrands of ten-dimensional SYM.

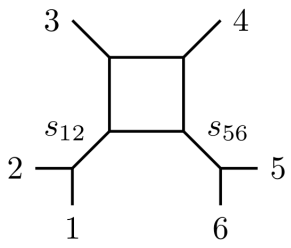

$$\frac{V_{12}T_{3,4,56}}{s_{12}s_{56}}$$

The superspace expressions encoding the integrands are in the cohomology of the pure spinor BRST charge, whose action on kinematic factors follows from simple equations of motion [11,12]. The cohomology requirement on scattering amplitudes tightly constrains the admissible combinations of superfields which, when supplemented by the required propagator structure of the amplitudes, empirically leads to unique answers.

The cohomology approach was successfully applied to assemble tree amplitudes from its cubic graphs [13,9]. The kinematic objects which describe individual subdiagrams share

[1] See [4,5] for reviews of the pure spinor formalism and [6] for a recent derivation of the BRST operator from first principles.

the symmetries of the associated color factors, leading to a manifestation of the BCJ duality [3] in tree amplitudes [14]. Their generalization to multiparticle superfields of SYM in [12] provides a superspace representation for any tree-level subdiagram in a one-loop amplitude. For example, the four-point box numerator can be written as $V_1 T_{2,3,4}$ while the six-point box in the above figure is represented by $V_{12} T_{3,4,56}$, where two of the superfields are exchanged by their multiparticle representatives. Hence, the leftover challenge boils down to fixing the irreducible n-gon diagram in the n-point one-loop amplitude using BRST invariance. Multiparticle superfields then allow to infer the structure of massive n-gons at higher multiplicity.

This paper is structured as follows. Section 2 reviews the diagrammatic construction of tree-level amplitudes based on BRST properties of the kinematic numerators in superspace. In section 3, we introduce a set of one-loop specific superfields as selected by the zero-mode saturation of the open superstring. They furnish the alphabet of BRST-covariant building blocks for any kinematic numerator in one-loop integrands. Their precise matching with box, pentagon and hexagon diagrams is dictated by the BRST algebra and explained in section 4. This leads to a superspace description of the hexagon anomaly [15] inherent to the chiral fermions of ten-dimensional SYM.

Even though BRST invariance serves as a driving force to determine the kinematic numerators, it is not manifest at the level of individual diagrams of the local integrands. Hence, we provide an alternative representation in section 5 where the propagators are reorganized such that any kinematic factor is manifestly BRST *pseudo-invariant* – meaning BRST closed up to anomaly effects [16]. These cohomology objects have been classified in [16] and shown to obey a rich network of relations under permutations of external legs and contractions with momenta. Representations with manifest BRST properties obscure locality but allow to check cyclic symmetry of the integrated amplitudes in superspace – again up to the hexagon anomaly.

Finally, section 6 is devoted to the BCJ duality. The five-point integrand is shown to obey all kinematic Jacobi relations, and the corresponding type IIA/B supergravity amplitudes are presented as a corollary – in lines with the field theory limit of the closed superstring. However, the six-point amplitude suffers from obstructions to satisfy the BCJ duality whose precise form might signal a subtle relation to the anomaly.

For any superspace numerator presented in this work, the gluon- and gluino components are explicitly accessible by combining the known θ expansions of the superfields [17] with the component prescription $\langle \lambda^3 \theta^5 \rangle = 1$ of pure spinor superspace [7]. On the basis of its automatization in [18], the gluon components of any kinematic factor in the amplitude representations of section 5 are available on the website [19].

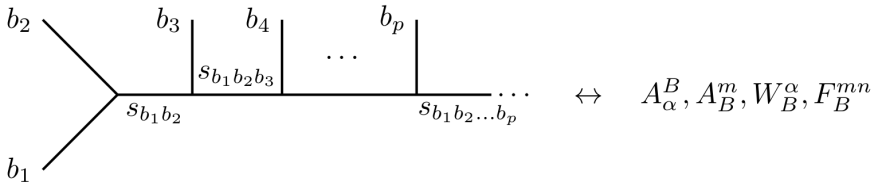

Fig. 1 The correspondence of cubic graphs and the BRST blocks with multiparticle label $B = b_1 b_2 \ldots b_p$. For the unintegrated vertex $V^B = \lambda^\alpha A^B_\alpha$, this mapping implies that the BRST variation of cubic graph numerators cancels propagators and allows the construction of tree-level amplitudes which are BRST invariant.

2. Tree-level cohomology construction of SYM amplitudes

In this section, we review the pure spinor cohomology derivation of the tree-level amplitudes of SYM theory [13,9] using the BRST block techniques of [12]. This will prove useful to undertake the analogous construction of one-loop amplitudes.

2.1. BRST-covariant building blocks from the pure spinor string

The tree-level amplitude among n massless open superstring states is encoded in iterated integrals along the boundary of a worldsheet of disk topology parametrized by real z_i. The prescription in the pure spinor formalism is given by

$$\mathcal{A}_n^{\rm tree} = \int \prod_{j=2}^{n-2} dz_j \langle V^1(z_1)\, U^2(z_2)\, \ldots\, U^{n-2}(z_{n-2})\, V^{n-1}(z_{n-1})\, V^n(z_n)\rangle \qquad (2.1)$$

where $V(z)$ and $U(z)$ are the vertex operators for the gluon super-multiplet

$$V^i = \lambda^\alpha A^i_\alpha, \qquad U^i = \partial\theta^\alpha A^i_\alpha + \Pi_m A^m_i + d_\alpha W^\alpha_i + \frac{1}{2} N_{mn} F^{mn}_i \ , \qquad (2.2)$$

and $[A_\alpha, A^m, W^\alpha, F_{mn}]$ are the ten-dimensional superfields of $\mathcal{N} = 1$ SYM [11]. They are contracted into the spinorial ghost λ^α subject to the pure spinor constraint $\lambda\gamma^m\lambda = 0$, and $[\partial\theta^\alpha, \Pi_m, d_\alpha, N_{mn}]$ are conformal primaries of weight $h = 1$, see [20] for their OPEs.

The correlation function in (2.1) is determined by the OPEs among the vertices, $V(z)U(w)$ and $U(z)U(w)$. Based on the experience from four- to six-point computations [21], the general solution to this problem was argued in [12] to be captured by multiparticle superfields $[A^B_\alpha, A^m_B, W^\alpha_B, F^B_{mn}]$. As shown in [12], they generalize the standard (single-particle) SYM superfields of [11] and can be interpreted as representing a multiperipheral tree level subdiagram with an off-shell leg, see fig. 1. The on-shell legs b_j are collected in multiparticle labels $B = b_1 b_2 \ldots b_p$, usually denoted by capital Latin letters.

More precisely, kinematic factors of the n-point string amplitude at tree level can always be written in terms of multiparticle vertex operators,

$$V^B \equiv \lambda^\alpha A^B_\alpha \ , \quad U_B \equiv \partial\theta^\alpha A^B_\alpha + \Pi_m A^m_B + d_\alpha W^\alpha_B + \frac{1}{2} N_{mn} F^{mn}_B \ . \tag{2.3}$$

The simplest two-particle instance reads

$$V^{12} \equiv \frac{1}{2}\big[V_2(k^2\cdot A^1) + A^2_m(\gamma^m W^1)_\alpha - (1\leftrightarrow 2)\big] \,, \tag{2.4}$$

and a recursive prescription for cases with three and more particles is given in [12]. The resulting multiparticle fields $[A^B_\alpha, A^m_B, W^\alpha_B, F^{mn}_B]$ satisfy Lie-symmetries such as

$$V^{12} = -V^{21}, \quad V^{123} = -V^{213}, \quad V^{123} + V^{231} + V^{312} = 0 \,, \tag{2.5}$$

in lines with the dual color tensors f^{12a} and $f^{12a}f^{a3b}$ [3].

Multiparticle vertices build up by iterating OPEs of schematic form $U_A U_B \to U_C$ and $V_A U_B \to V_C$. Once the conformal fields $[\partial\theta^\alpha, \Pi_m, d_\alpha, N_{mn}]$ in (2.1) are integrated out along these lines, the most general kinematic pattern in superstring tree amplitudes is furnished by $V_A V_B V_C$. Their ghost number three is compatible with the component prescription [7]

$$\langle (\lambda\gamma^m\theta)(\lambda\gamma^n\theta)(\lambda\gamma^p\theta)(\theta\gamma_{mnp}\theta)\rangle = 2880 \ . \tag{2.6}$$

Since the open superstring reduces to ten-dimensional $\mathcal{N}=1$ SYM in the field-theory limit $\alpha'\to 0$ [22], these same ingredients of the form $V_A V_B V_C$ suffice to write down SYM amplitudes. Furthermore, supersymmetry of the string amplitudes in the pure spinor formalism is a consequence of BRST invariance independently of the α' order, so the SYM amplitudes must also be BRST invariant.

The above reasoning led to the conjecture in [13] that the n-point tree amplitudes of SYM could be obtained by requiring BRST invariance of linear combinations of $V_A V_B V_C$ with the appropriate kinematic pole structure. This conjecture eventually led to a recursive algebraic method for the n-point SYM tree amplitude in [9], but it will be convenient to recall the diagrammatic construction suggested in [13] since it will be generalized to one-loop below.

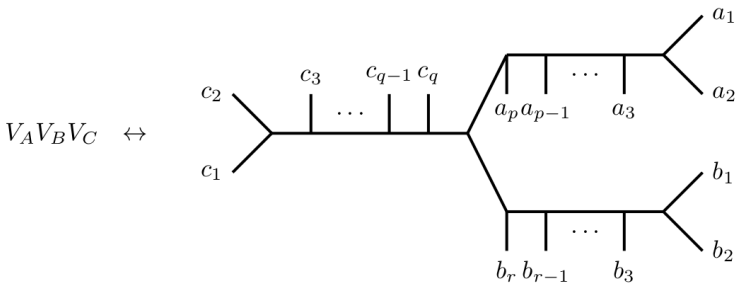

Fig. 2 On-shell diagrams represented by $V_AV_BV_C$ connect three off-shell subdiagrams. Propagators such as $s_{a_1a_2}$ and $s_{a_1a_2a_3}$ are suppressed on the left-hand side.

2.2. BRST variations and diagrammatic interpretation

At the level of SYM superfields, the BRST operator acts as a fermionic derivative,

$$Q = \lambda^\alpha D_\alpha \ , \quad D_\alpha \equiv \frac{\partial}{\partial\theta^\alpha} + \frac{1}{2}k_m(\gamma^m\theta)_\alpha \ . \tag{2.7}$$

The multiparticle equations of motion for A^B_α [12] imply covariant BRST variations forV_B,

$$QV_{12} = s_{12}V_1V_1 \ , \quad QV_{123} = (s_{123} - s_{12})V_{12}V_3 + s_{12}(V_1V_{23} + V_{13}V_2) \ , \tag{2.8}$$

see [12] for multiparticle generalizations. The Mandelstam invariants in (2.8) are defined by

$$s_{ij} \equiv (k_i \cdot k_j) = \frac{1}{2}(k_i + k_j)^2 \ , \quad s_{i_1i_2\ldots i_p} \equiv \frac{1}{2}(k_{i_1} + k_{i_2} + \ldots + k_{i_p})^2 \tag{2.9}$$

and guide the diagrammatic interpretation shown in fig. 1. For example, the variation $QV_{12} = s_{12}V_1V_2$ suggests to associate V_{12} with a propagator s_{12}^{-1}. The latter in turn describes a cubic vertex with on-shell particles 1 and 2 as well as an off-shell leg carrying the overall momentum $k_{12} \equiv k_1 + k_2$. Higher-multiplicity $V_{12\ldots p}$ have analogous BRST variations with Mandelstam invariants $s_{12\ldots j}$, $j = 2, 3, \ldots, p$, so they are the natural superspace representatives of cubic subdiagrams with these propagators. The resulting multiperipheral tree level subdiagrams with a terminal off-shell leg are depicted in fig. 1. The trilinears $V_AV_BV_C$ selected by the above string theory prescription allows to connect the three off-shell legs through an additional vertex and to form an on-shell tree level diagram, see fig. 5.

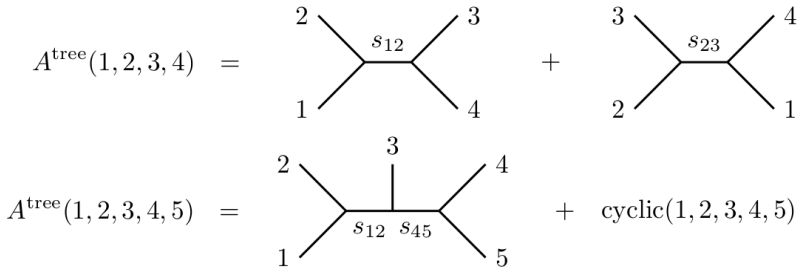

Fig. 3 The four- and five-point tree amplitudes represented in terms of cubic graphs.

2.3. Tree-level SYM amplitudes from the cohomology of pure spinor superspace

The color-ordered tree-level SYM amplitudes can be organized in terms of cubic on-shell graphs capturing their kinematic pole structure [3],

$$A^{\rm tree}(1,2,\ldots,n) = \sum_{\Gamma_i} \frac{N_i}{\prod_k P_{k,i}} \ . \tag{2.10}$$

The sum encompasses all cubic diagrams Γ_i compatible with the color ordering, and $P_{k,i}$ denote their corresponding propagators, see fig. 3 for four- and five-point examples. The kinematic numerators N_i carry the polarization dependence and will be specified below.

The pure spinor cohomology method of [9] exploits the dictionary of fig. 2 between cubic diagrams and superfields to associate trilinear $V_A V_B V_C$ with each numerators N_i in (2.10). The BRST-covariant properties of the BRST blocks (see (2.8) and [12]) guarantee that these superspace numerators satisfy the necessary condition for BRST invariance:

$$\textit{each term of } QN_i \textit{ must have a factor of } P_{k,i} \textit{ with } k = 1,2,\ldots,n-3. \tag{2.11}$$

Otherwise, the BRST variation of the amplitude would have a nonzero residue at the simultaneous pole $\prod_k P_{k,i}$ and could not vanish.

One can check that the following mapping between cubic graphs and pure spinor superspace expressions leads to BRST-invariant four- and five-point amplitudes:

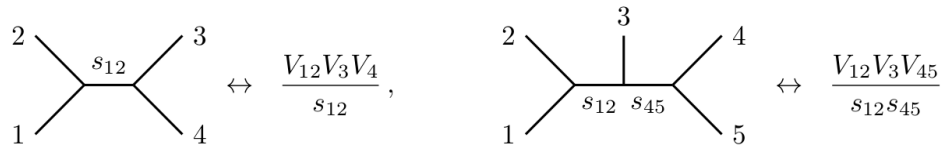

Using these mappings the four- and five-point amplitudes displayed in fig. 3 become

$$\begin{aligned} A^{\rm tree}(1,2,3,4) &= \frac{\langle V_{12}V_3V_4\rangle}{s_{12}} + \frac{\langle V_{23}V_4V_1\rangle}{s_{23}} \\ A^{\rm tree}(1,2,3,4,5) &= \frac{\langle V_{12}V_3V_{45}\rangle}{s_{12}s_{45}} + \text{cyclic}(1,2,3,4,5) \ . \end{aligned} \tag{2.12}$$

BRST invariance follows from the cancellation of the propagators e.g.

$$\frac{QV_{12}V_3V_4}{s_{12}} = V_1V_2V_3V_4\,, \quad \frac{QV_{12}V_3V_{45}}{s_{12}s_{45}} = \frac{V_1V_2V_3V_{45}}{s_{45}} + \frac{V_{12}V_3V_4V_5}{s_{12}}\,, \tag{2.13}$$

and both terms in the right-hand side of the five-point diagram can cancel against further diagrams which share one of the propagators s_{12}, s_{45}. Note that any pure spinor superspace numerator $\langle V_A V_B V_C\rangle$ is a *local* expression of polarizations and momenta.

Higher-point amplitudes can be similarly obtained using vertices V_B of higher multiplicity. SYM tree amplitude up to seven points can be found in [13], and the n-point solution is presented in [9] based on a recursive method. Furthermore, explicit component expansions of SYM trees up to multiplicity eight can be found in the website [19].

Note that the assignment of superfields to a cubic graph is not unique. By choosing different vertices to play the role of the center of fig. 2, one can arrive at three representations for the following five-point diagram:

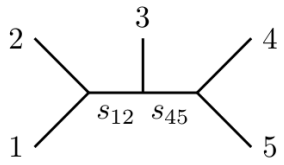

$$\leftrightarrow \quad \frac{V_{123}V_4V_5}{s_{12}s_{45}}\,, \quad \frac{V_{12}V_3V_{45}}{s_{12}s_{45}}\,, \quad \frac{V_{543}V_1V_2}{s_{12}s_{45}}$$

They differ by contact terms and have to be chosen coherently such as to render the resulting amplitude (2.10) BRST invariant. At tree level, a consistent choice consists of trilinears of the schematic form $V_{1\ldots}V_{n-1\ldots}V_n$. The legs of the integrated vertices $2, 3, \ldots, n-2$ in (2.1) are distributed along the ellipses of $V_{1\ldots}$ or $V_{n-1\ldots}$, and the single particle nature of V_n reflects the choice of worldsheet position $z_n \to \infty$. This is also a $(n-2)!$ basis of local tree level numerators found in [14] which satisfy the duality between color and kinematics.

As we will see in the next sections, similar ambiguities arise at one-loop and can be settled through the choice of unintegrated vertex operator V_1 such that the first particle one can only enter through V_B with $B = 1b_2b_3\ldots$.

3. One-loop cohomology construction of SYM integrands

In this section, one-loop string amplitude prescription will be used to propose kinematic building blocks in superspace for SYM one-loop integrands. This will be done in a similar diagrammatic fashion as reviewed for tree level amplitudes in the previous section.

3.1. Review of the four point amplitude

The four-point one-loop amplitudes of ten-dimensional SYM and supergravity were firstly determined in 1982 by Brink, Green and Schwarz by taking the field-theory limit of their superstring ancestors. Remarkably, the only contributing Feynman integral was found to be the box graph [22],

$$A(1,2,3,4) = \int \frac{d^D\ell}{(2\pi)^D} \frac{s_{12}s_{23}A^{\rm tree}(1,2,3,4)}{\ell^2(\ell-k_1)^2(\ell-k_{12})^2(\ell-k_{123})^2} \tag{3.1}$$

$$M_4 = \int \frac{d^D\ell}{(2\pi)^D} \frac{s_{12}s_{23}s_{13}M_4^{\rm tree}}{\ell^2(\ell-k_1)^2(\ell-k_{12})^2(\ell-k_{123})^2} \ , \tag{3.2}$$

where the ordering of particles in (3.1) refers to a single color–trace. The analogous pure spinor derivations have been performed in [23] resulting in superspace kinematic factors

$$s_{12}s_{23}A^{\rm tree}(1,2,3,4) = \langle V_1(\lambda\gamma_m W_2)(\lambda\gamma_n W_3)F_4^{mn}\rangle \tag{3.3}$$

$$s_{12}s_{23}s_{13}M_4^{\rm tree} = \langle |V_1(\lambda\gamma_m W_2)(\lambda\gamma_n W_3)F_4^{mn}|^2\rangle \ . \tag{3.4}$$

In the remainder of this paper, we develop systematic methods to determine their generalization at higher multiplicity, making either locality or BRST pseudo-invariance manifest. As a first step, the superfields in (3.3) will be generalized below to BRST-covariant building blocks suitable to represent non-trivial tree subdiagrams and ℓ^m-dependent parts.

3.2. BRST-covariant building blocks from the pure spinor prescription

The one-loop pure spinor amplitude prescription of [23] leads to a richer set of BRST-covariant building blocks when compared to the tree-level prescription. As explained in [16], the zero-mode saturation patterns following from different contributions from the b-ghost suggest that building blocks of arbitrary tensor ranks appear in the one-loop string amplitudes. More precisely, the superstring prescription for one-loop amplitudes is given by an integral over conformally inequivalent cylinder[2] diagrams with circumference t [23],

$$\mathcal{A}_n = \int_0^\infty dt \int\limits_{0\le {\rm Im}\, z_i \le {\rm Im}\, z_{i+1}\le t} dz_2\, dz_3\, \ldots\, dz_n \langle \int d^2w\, b(w)\mu\, \mathcal{Z}\, V^1(z_1)\, U^2(z_2)\, \ldots\, U^n(z_n)\rangle \ . \tag{3.5}$$

[2] For the purpose of deriving single-trace color-ordered SYM amplitudes, we neglect the world-sheet topologies beyond the planar cylinder even though they play an important role in string theory for the cancellation of anomalies and divergences [24].

In contrast to the tree-level prescription (2.1), only one vertex operator V^1 appears in the unintegrated picture whereas $n-1$ vertices U^j are integrated along the cylinder boundary parametrized by purely imaginary z_j. The b-ghost, the various picture changing operators collectively denoted by $\mathcal{Z}$ and the Beltrami differencial μ are explained in [23], and the subsequent discussion only requires the schematic form of their zero-mode structure: Among the worldsheet fields of conformal weight one, zero-modes of $d_\alpha d_\beta N^{mn}$ must necessarily by saturated by the integrated vertices, regardless of the contribution from b and $\mathcal{Z}$. Given the single particle integrated vertex (2.2), this mechanism gives rise to the superfields $W_2^\alpha W_3^\beta F_4^{mn}$ in the four point amplitude (3.3).

At higher multiplicity, the correlator in (3.5) is determined by a cascade of OPEs among multiparticle vertices of schematic form $U_A U_B \to U_C$ and $V_A U_B \to V_C$. The expression (2.3) for their integrated version identifies the multiparticle fields $W_A^\alpha W_B^\beta F_C^{mn}$ along with the zero-modes $d_\alpha d_\beta N^{mn}$. Their two-particle representatives beyond V_{12} in (2.4) are given by

$$\begin{aligned} A_m^{12} &= \frac{1}{2}\Big[A_p^1 F_{pm}^2 - A_m^1(k^1\cdot A^2) + (W^1\gamma_m W^2) - (1\leftrightarrow 2)\Big] \\ W_{12}^\alpha &= \frac{1}{4}(\gamma^{mn}W^2)^\alpha F_{mn}^1 + W_2^\alpha(k^2\cdot A^1) - (1\leftrightarrow 2) \\ F_{mn}^{12} &= F_{mn}^2(k^2\cdot A^1) + F_{[m}^{2\ p}F_{n]p}^1 + k_{[m}^{12}(W_1\gamma_{n]}W_2) - (1\leftrightarrow 2) \end{aligned} \tag{3.6}$$

with $k_{12}^m \equiv k_1^m + k_2^m$, and generalizations to higher multiplicity can be found in [12]. The unique tensor structure combining the superfields $W_A^\alpha W_B^\beta F_C^{mn}$ to a ghost-number-two expression as required by the $\langle\lambda^3\theta^5\rangle = 1$ prescription [7] is given by the scalar

$$T_{A,B,C} \equiv \frac{1}{3}(\lambda\gamma_m W_A)(\lambda\gamma_n W_B)F_C^{mn} + (C\leftrightarrow B,A)\ . \tag{3.7}$$

It is symmetric under exchange of the slots A,B,C and generalizes the four–point kinematic factor in (3.3) to incorporate multiparticle tree-level subdiagrams.

The five- and six point amplitudes presented in the following also involve vector and symmetric tensor building blocks

$$T_{A,B,C,D}^m \equiv \big[T_{A,B,C}A_D^m + (D\leftrightarrow C,B,A)\big] + W_{A,B,C,D}^m \tag{3.8}$$

$$T_{A,B,C,D,E}^{mn} \equiv T_{A,B,C,D}^m A_E^n + W_{A,B,C,D}^n A_E^m + (E\leftrightarrow D,C,B,A)\ . \tag{3.9}$$

They stem from additional saturations of Π^m zero-modes from the integrated vertices (2.3) leaving behind the multiparticle superfield A_B^m. However, absorption of Π^m also involves another b-ghost sector which is represented through the shorthand

$$W^m_{A,B,C,D} \equiv \frac{1}{12}(\lambda\gamma_n W_A)(\lambda\gamma_p W_B)(W_C\gamma^{mnp}W_D) + (A,B|A,B,C,D)\ . \tag{3.10}$$

The notation $(A_1,\ldots,A_p\,|\,A_1,\ldots,A_n)$ instructs to sum over all possible ways to choose p elements $A_1,A_2,\ldots,A_p$ out of the set $\{A_1,\ldots,A_n\}$, for a total of $\binom{n}{p}$ terms.

Similar to the BRST variation (2.8) of tree-level constituents V_B, the one-loop building blocks (3.7) to (3.9) transform covariantly under Q [12], e.g.

$$\begin{aligned}
QT_{1,2,3} &= 0\ , \quad QT_{12,3,4} = s_{12}(V_1T_{2,3,4} - V_2T_{1,3,4})\\
QT_{12,34,5} &= s_{12}(V_1T_{2,34,5} - V_2T_{1,34,5}) + s_{34}(V_3T_{12,4,5} - V_4T_{12,3,5})\\
QT_{123,4,5} &= (s_{123}-s_{12})(V_{12}T_{3,4,5} - V_3T_{12,4,5})\\
&\quad + s_{12}(V_1T_{23,4,5} + V_{13}T_{2,4,5} - V_{23}T_{1,4,5} - V_2T_{13,4,5})\ .
\end{aligned} \tag{3.11}$$

The variation of vectors and tensors additionally involves terms proportional to k_i^m where the vector index is carried by a momentum:

$$\begin{aligned}
QT^m_{1,2,3,4} &= k_1^m V_1 T_{2,3,4} + (1\leftrightarrow 2,3,4)\\
QT^m_{12,3,4,5} &= s_{12}(V_1T^m_{2,3,4,5} - V_2T^m_{1,3,4,5}) + k_{12}^m V_{12}T_{3,4,5} + \big[k_3^m V_3 T_{12,4,5} + (3\leftrightarrow 4,5)\big]\\
QT^{mn}_{1,2,3,4,5} &= \big[2k_1^{(m}V_1T^{n)}_{2,3,4,5} + (1\leftrightarrow 2,3,4,5)\big] + \delta^{mn}Y_{1,2,3,4,5}\ .
\end{aligned} \tag{3.12}$$

The last term in the tensor variation was firstly considered in the pure spinor description of the would-be hexagon anomaly of the superstring[3] in [26]

$$Y_{A,B,C,D,E} \equiv \frac{1}{2}(\lambda\gamma^m W_A)(\lambda\gamma^n W_B)(\lambda\gamma^p W_C)(W_D\gamma_{mnp}W_E)\ , \tag{3.13}$$

it is totally symmetric in $A,B,\ldots,E$ by the pure spinor constraint. Generalizations to higher rank were introduced in [16]. Another building block $J_{1|2,3,4,5}$ [16] capturing subtleties of the six-point anomaly in pure spinor superspace will be discussed in section 4.4.

[3] As shown by Green and Schwarz in 1984, the hexagon anomaly cancels in the superstring for the gauge group $SO(32)$ [25].

3.3. The diagrammatic structure of one-loop amplitudes

Since string theory reduces to field theory in the $\alpha' \to 0$ limit, the above building blocks together with V_A should suffice to describe SYM one-loop amplitudes. In the subsequent, we will focus on the superspace integrand $A(1,2,3,\ldots,n|\ell)$ governing the integrated color ordered single-trace[4] amplitude $A(1,2,3,\ldots,n)$ via

$$A(1,2,3,\ldots,n) = \int \frac{d^D\ell}{(2\pi)^D} \langle A(1,2,3,\ldots,n|\ell)\rangle \ . \tag{3.14}$$

Similar to the cubic graph organization of the tree-level amplitude (2.10), also one-loop SYM amplitudes can be described in terms cubic graphs Γ_i, [28],

$$A(1,2,3,\ldots,n|\ell) = \sum_{\Gamma_i} \frac{N_i(\ell)}{\prod_k P_{k,i}(\ell)} \ . \tag{3.15}$$

The sum over cubic diagrams Γ_i ranges from boxes to n-gons whose external tree-level subdiagrams respect the color ordering on the left-hand side. The no-triangle property [27] of maximally supersymmetric SYM excludes triangles, bubbles and tadpoles. The superspace numerators $N_i(\ell)$ and the propagators $P_{k,i}(\ell)$ now depend on the loop momentum ℓ_m, in addition to the external kinematics. Moreover, supersymmetry bounds the powers of loop momenta ℓ in the numerators $N_i(\ell)$ of a p-gon diagram to be $\leq p-4$.

The observations above will be exploited to propose a novel supersymmetric description of one-loop SYM integrands following two steps. Firstly, we propose mappings between n-gon numerators and pure spinor superspace expressions such as $V_A T_{B,C,D}$ and generalizations to higher rank. This mapping is naturally suggested by the propagators cancelled by the BRST-covariant variation of the building blocks,

$$\textit{each term of } QN_i(\ell) \textit{ must have a factor of } P_{k,i}(\ell) \textit{ with } k = 1,2,\ldots,n, \tag{3.16}$$

generalizing the tree-level counterpart (2.11) to ℓ-dependent $P_{k,i}$. And secondly, an overall BRST-invariant superspace expression compatible with the cubic graphs in (3.15) must be assembled with the help of the mappings proposed in step one.

Even though the construction is carried out in a ten-dimensional setup, the momenta and external polarizations can still be restricted to lower dimensions [2]. The one-loop integrals in [28] are UV-finite if $D < 8$, the dimensional reduction [2] of our results is then expected to integrate to SYM amplitudes in this dimension. In $D = 4$, for instance, the subsequent integrands are checked[5] to reproduce MHV amplitudes with the right unitarity cuts.

[4] At one-loop, SYM subamplitudes associated with double-trace color factors can be recovered through linear combinations of single-trace subamplitudes [27].

[5] We thank Song He for checking it.

4. Local SYM superspace integrands at four, five and six points

In this section the cubic-graph organization of the SYM integrands (3.14) will be exploited in connection with their BRST pseudo-invariance inherited from the pure spinor superstring description. Using the building blocks reviewed in the previous section, manifestly local integrands will be constructed following BRST cohomology arguments.

4.1. Local form of the one-loop four-point SYM integrand

Let us rewrite the four-point SYM integrand using the above superfield definitions in order to appreciate the natural structure of its higher-point generalizations. The integrand of the color-ordered amplitude contains only one box:

$A(1,2,3,4|\ell)$ =

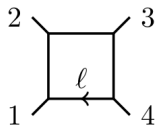

and its pure spinor superspace expression is given by

$$A(1,2,3,4|\ell) = \frac{V_1 T_{2,3,4}}{\ell^2(\ell-k_1)^2(\ell-k_{12})^2(\ell-k_{123})^2}\,. \tag{4.1}$$

This simple example provides the essential intuition on setting up a mapping between boxes and superspace expressions. It will be seen below that a general higher-point box with corners encoded by multiparticle labels A, B, C and D (having the structure of cubic-graph tree subamplitudes) is mapped to $V_A T_{B,C,D}$.

4.2. Local form of the one-loop five-point SYM integrand

In the color-ordered SYM five-point one-loop integrand the only cubic graphs compatible with the no-triangle property are boxes and pentagons:

$A(1,2,3,4,5|\ell)$ =

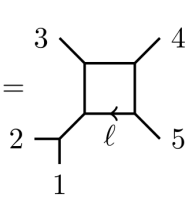

+ cyclic(12345) +

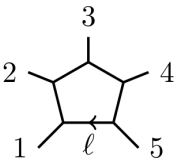

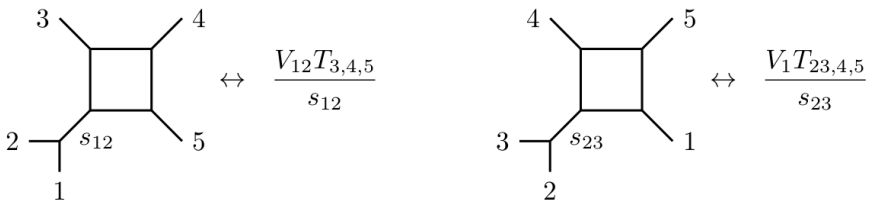

Fig. 4 The explicit superspace representation of the five-point box numerators. The form of the numerators depends on the location of leg 1, and the origin of this difference is due to the string one-loop amplitude prescription (3.5) fixing the position of its first vertex operator V_1.

Hence, we split its integrand according to box and pentagon contributions

$$A(1,2,3,4,5|\ell) = A_{\rm box}(1,2,3,4,5) + A_{\rm pent}(1,2,3,4,5|\ell)\ , \tag{4.2}$$

where $A_{\rm box}(\ldots)$ is independent on ℓ and $A_{\rm pent}(\ldots)$ carries at most linear ℓ-dependence. For the numerators of the boxes, the requirement (3.16) yields a natural pure spinor superspace representation seen in fig. 4. Since triangles in the BRST variation cannot be compensated by any other p-gon diagram with $p \geq 4$, their BRST variation must cancel the propagator $s_{i,i+1}$ of their external tree-level subdiagram:

$$\begin{aligned} A_{\rm box}(1,2,3,4,5) = &\frac{V_{12}T_{3,4,5}}{(k_1+k_2)^2\ell^2(\ell-k_{12})^2(\ell-k_{123})^2(\ell-k_{1234})^2} \\ &+ \frac{V_1T_{23,4,5}}{(k_2+k_3)^2\ell^2(\ell-k_1)^2(\ell-k_{123})^2(\ell-k_{1234})^2} \\ &+ \frac{V_1T_{2,34,5}}{(k_3+k_4)^2\ell^2(\ell-k_1)^2(\ell-k_{12})^2(\ell-k_{1234})^2} \\ &+ \frac{V_1T_{2,3,45}}{(k_4+k_5)^2\ell^2(\ell-k_1)^2(\ell-k_{12})^2(\ell-k_{123})^2} \\ &+ \frac{V_{51}T_{2,3,4}}{(k_1+k_5)^2(\ell-k_1)^2(\ell-k_{12})^2(\ell-k_{123})^2(\ell-k_{1234})^2}\ . \end{aligned} \tag{4.3}$$

These expressions can be thought of as descending from a string calculation where particle one enters through an unintegrated vertex V_1. That is why the first leg always enters in the form $V_{1\ldots}$ and ambiguities such as $V_1T_{23,4,5} \leftrightarrow V_{23}T_{1,4,5}$ do not arise.

On the other hand, the pentagon numerator $N^{(5)}_{1|2,3,4,5}(\ell)$ in

$$A_{\rm pent}(1,2,3,4,5|\ell) = \frac{N^{(5)}_{1|2,3,4,5}(\ell)}{\ell^2(\ell-k_1)^2(\ell-k_{12})^2(\ell-k_{123})^2(\ell-k_{1234})^2} \tag{4.4}$$

must be designed such that ℓ-dependent propagators cancel in its BRST variation. This interlocks the vector $\ell_m V_1 T^m_{2,3,4,5}$ with the scalars in

$$N^{(5)}_{1|2,3,4,5}(\ell) \equiv \ell_m V_1 T^m_{2,3,4,5} + \frac{1}{2}\big[V_{12}T_{3,4,5} + (2 \leftrightarrow 3,4,5)\big] + \frac{1}{2}\big[V_1 T_{23,4,5} + (2,3|2,3,4,5)\big]\,. \tag{4.5}$$

In contrast to the box numerators of the form $V_A T_{B,C,D}$, the pentagon numerator (4.5) depends on the ordering of the external legs $2,3,4,5$ through the signs in the scalar part. The variations (3.11) and (3.12) of the scalar and vectorial building blocks imply that

$$\begin{aligned} QN^{(5)}_{1|2,3,4,5}(\ell) = {} & \frac{1}{2}V_1V_2T_{3,4,5}\big[(\ell-k_{12})^2-(\ell-k_1)^2\big] + \frac{1}{2}V_1V_3T_{2,4,5}\big[(\ell-k_{123})^2-(\ell-k_{12})^2\big] \\ & + \frac{1}{2}V_1V_4T_{2,3,5}\big[(\ell-k_{1234})^2-(\ell-k_{123})^2\big] + \frac{1}{2}V_1V_5T_{2,3,4}\big[\ell^2-(\ell-k_{1234})^2\big] \end{aligned} \tag{4.6}$$

is compatible with (3.16) and precisely cancels the BRST variation of the boxes in (4.3):

$$\begin{aligned} QA_{\rm box}(1,2,3,4,5) = {} & \frac{V_1V_2T_{3,4,5}}{2\ell^2(\ell-k_{123})^2(\ell-k_{1234})^2}\left(\frac{1}{(\ell-k_{12})^2}-\frac{1}{(\ell-k_1)^2}\right) \\ & + \frac{V_1V_3T_{2,4,5}}{2\ell^2(\ell-k_1)^2(\ell-k_{1234})^2}\left(\frac{1}{(\ell-k_{123})^2}-\frac{1}{(\ell-k_{12})^2}\right) \\ & + \frac{V_1V_4T_{2,3,5}}{2\ell^2(\ell-k_1)^2(\ell-k_{12})^2}\left(\frac{1}{(\ell-k_{1234})^2}-\frac{1}{(\ell-k_{123})^2}\right) \\ & + \frac{V_1V_5T_{2,3,4}}{2(\ell-k_1)^2(\ell-k_{12})^2(\ell-k_{123})^2}\left(\frac{1}{\ell^2}-\frac{1}{(\ell-k_{1234})^2}\right)\,. \end{aligned} \tag{4.7}$$

Hence, the interplay between boxes and pentagons renders the superspace integrand (4.2) BRST invariant, $QA(1,2,3,4,5|\ell)=0$. Note the factor of $\frac{1}{2} = \frac{s_{ij}}{(k_i+k_j)^2}$ by the convention (2.9) for Mandelstam invariants. In section 5.2, we will present an alternative representation of the five-point amplitude where BRST invariance is manifest. And it will be shown in appendix A that the integrand (4.2) is confirmed by the field-theory limit of the superstring amplitude.

4.3. Shorthand notations

The length of the five-point box contribution in (4.3) and the superspace presentation of the pentagon numerator (4.5) motivate to introduce a compact notation for both numerators and ℓ-dependent propagators before addressing the six–point amplitude.

4.3.1. ℓ-dependent propagators

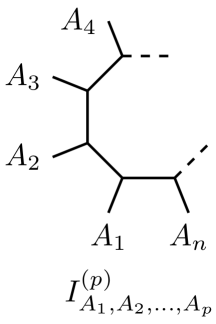

A general p-gon diagram involves multiparticle tree subdiagrams $A_1, A_2, \ldots, A_p$ on its corners and we define a shorthand $I^{(p)}_{A_1,A_2,\ldots,A_p}$ for the p propagators which depend on ℓ. The figure on the right does not yet specify the position of the loop momentum ℓ in the diagram. The five-point amplitude (4.2) was presented with uniform propagators $\ell, (\ell - k_1)^2, \ldots, (\ell - k_{1234})^2$, i.e. without any shifts $\ell \to \ell + k_i$ of integration variables between different diagrams. This was crucial to demonstrate BRST invariance at the level of the integrand. Hence, we pick the following convention to freeze the freedom of redefining ℓ:

the only ℓ-dependent propagators in $A(1, 2, \ldots, n|\ell)$ are $(\ell - k_{12\ldots j})^2$ with $0 \leq j \leq n-1$. (4.8)

The explicit formula for the $I^{(p)}_{A_1,A_2,\ldots,A_p}$ in the above figure therefore requires to specify the position of leg 1 within the first massive corner $A_1 \equiv B1C$:

$$I^{(p)}_{B1C,A_2,A_3,\ldots,A_p} \equiv \frac{1}{(\ell - k_{1C})^2(\ell - k_{1CA_2})^2(\ell - k_{1CA_2A_3})^2 \ldots (\ell - k_{1CA_2A_3\ldots A_p})^2} \ . \quad (4.9)$$

Whenever the first corner A_1 does not contain particle n and starts with particle 1, we have $B = \emptyset$ and obtain $(\ell - k_{1CA_2A_3\ldots A_p})^2 = \ell^2$ by momentum conservation, e.g.

$$I^{(4)}_{12,34,5,6} \equiv \frac{1}{\ell^2(\ell - k_{12})^2(\ell - k_{1234})^2(\ell - k_{12345})^2} \ . \quad (4.10)$$

However, in cases with $B \neq \emptyset$ where a massive corner encompasses both legs 1 and n, absence of the ℓ^2 propagator will later on play a crucial role for the hexagon anomaly, e.g.

$$I^{(5)}_{61,2,3,4,5} \equiv \frac{1}{(\ell - k_1)^2(\ell - k_{12})^2(\ell - k_{123})^2(\ell - k_{1234})^2(\ell - k_{12345})^2} \ . \quad (4.11)$$

4.3.2. Box and pentagon numerators

The form of the box numerators in (4.3) strongly suggests the general pattern when arbitrary tree subdiagrams are attached to the four corners. Multiparticle labels such as $A = a_1 a_2 \ldots a_p$ allow for the following general formula,

$$N^{(4)}_{A|B,C,D} \equiv V_A T_{B,C,D} \ , \quad (4.12)$$

with $T_{B,C,D}$ given by (3.7). The interpretation of all the multiparticle superfields in $V_A T_{B,C,D}$ as off-shell tree subdiagrams as seen in fig. 1 leads to the desired box diagram for the right-hand side of (4.12).

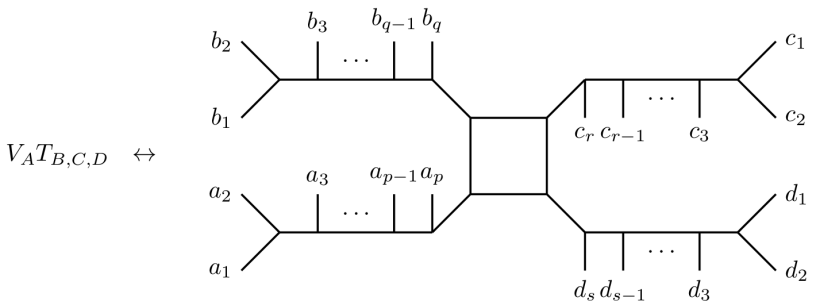

Fig. 5 On-shell diagrams represented by $V_A T_{B,C,D}$ connect four off-shell subdiagrams. Propagators such as $s_{a_1 a_2}$ and $s_{a_1 a_2 a_3}$ are suppressed on the left-hand side.

According to the BRST covariant transformation of both V_A and $T_{B,C,D}$ – see (2.8) and (3.11) for examples – the expression (4.12) for box numerators is compatible with both (3.16) and the no-triangle property.

A uniform description of pentagon numerators can be achieved using the bracketing convention of BRST blocks explained in appendix A of [12]: Multiparticle indices $B = b_1 b_2 \ldots b_p$ associated with the local superfields $[A^B_\alpha, A^m_B, W^\alpha_B, F^{mn}_B]$ can be combined through an antisymmetric bracket $[B_1, B_2] \to B_3$, e.g.

$$V_{[1,2]} \equiv V_{12} \ , \quad V_{[12,3]} \equiv V_{123} \ , \quad V_{[123,4]} \equiv V_{1234} \ , \quad V_{[12,34]} \equiv V_{1234} - V_{1243} \ . \tag{4.13}$$

The diagram associated with the superfield $V_{[B_1,B_2]}$ is obtained by connecting the off-shell legs of B_1, B_2 through a cubic vertex,

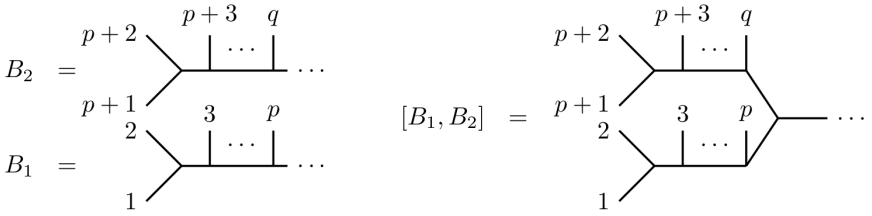

In this convention, the five-point pentagon numerator (4.5) can be generalized to

$$\begin{aligned} N^{(5)}_{A|B,C,D,E}(\ell) \equiv \ell_m V_A T^m_{B,C,D,E} + \frac{1}{2}\big[V_{[A,B]} T_{C,D,E} + (B \leftrightarrow C,D,E)\big] \\ + \frac{1}{2}\big[V_A T_{[B,C],D,E} + (B,C|B,C,D,E)\big] \, . \end{aligned} \tag{4.14}$$

In contrast to the box numerator (4.12), this pentagon numerator depends on the ordering of the external trees B, C, D, E. The antisymmetric components such as

$$N^{(5)}_{A|B,C,D,E}(\ell) - N^{(5)}_{A|C,B,D,E}(\ell) = N^{(4)}_{A|[B,C],D,E} \tag{4.15}$$

reproduce box numerators (4.12) with a bracket $[B, C]$ as exemplified in (4.13) in one of the multiparticle slots. This is in lines with the BCJ duality between color and kinematics [3] discussed in section 6.

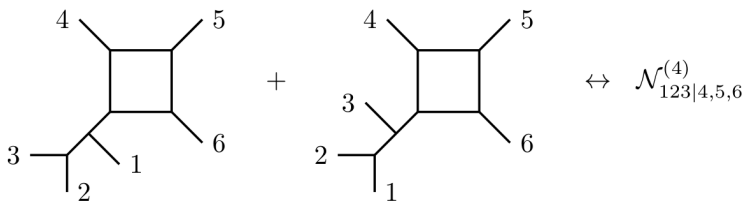

Fig. 6 The pure spinor superspace description of two one-mass box graphs in the six-point amplitude is compactly captured by Berends–Giele numerators such as $\mathcal{N}^{(4)}_{123|4,5,6}$ defined in (4.17). The expansion of the above superspace expression is given in (4.21).

4.3.3. Representing external tree-level propagators

In order to compactly describe the ℓ-independent propagators in the external tree-level subdiagrams, it is convenient to use the notation

$$\mathcal{N}^{(p)}_{12|3,\ldots,p+1} \equiv \frac{N^{(p)}_{12|3,\ldots,p+1}}{s_{12}} \ , \qquad \mathcal{N}^{(p)}_{1|23,\ldots,p+1} \equiv \frac{N^{(p)}_{1|23,\ldots,p+1}}{s_{23}} \tag{4.16}$$

for five-point boxes and six-point pentagons. Likewise, the presentation of six-point boxes benefits from the shorthands such as

$$\begin{aligned} \mathcal{N}^{(4)}_{123|4,5,6} &\equiv \frac{N^{(4)}_{123|4,5,6}}{s_{12}s_{123}} + \frac{N^{(4)}_{321|4,5,6}}{s_{23}s_{123}} \ , \qquad \mathcal{N}^{(4)}_{12|34,5,6} \equiv \frac{N^{(4)}_{12|34,5,6}}{s_{12}s_{34}} \\ \mathcal{N}^{(4)}_{1|234,5,6} &\equiv \frac{N^{(4)}_{1|234,5,6}}{s_{23}s_{234}} + \frac{N^{(4)}_{1|432,5,6}}{s_{34}s_{234}} \ , \qquad \mathcal{N}^{(4)}_{1|23,45,6} \equiv \frac{N^{(4)}_{1|23,45,6}}{s_{23}s_{45}} \ . \end{aligned} \tag{4.17}$$

They streamline the pairing of one-mass boxes and incorporate the concept of Berends–Giele currents [12], see fig. 6.

With the above shorthands, the five-point amplitude determined by (4.2) to (4.5) can be cast into the compact form

$$\begin{aligned} A(1,2,3,4,5|\ell) = N^{(5)}_{1|2,3,4,5}(\ell) I^{(5)}_{1,2,3,4,5} + \frac{1}{2}\Big[&\mathcal{N}^{(4)}_{12|3,4,5} I^{(4)}_{12,3,4,5} + \mathcal{N}^{(4)}_{1|23,4,5} I^{(4)}_{1,23,4,5} \\ &+ \mathcal{N}^{(4)}_{1|2,34,5} I^{(4)}_{1,2,34,5} + \mathcal{N}^{(4)}_{1|2,3,45} I^{(4)}_{1,2,3,45} + \mathcal{N}^{(4)}_{51|2,3,4} I^{(4)}_{51,2,3,4} \Big] \ . \end{aligned} \tag{4.18}$$

The six-point amplitude will now be presented along similar lines.

4.4. Local form of the one-loop six-point SYM integrand

The color-ordered six-point SYM integrand will be constructed in a local form following the propagator-cancellation principle (3.16) for all its numerators. Boxes, pentagons and the hexagon are analyzed separately to get an overview of their BRST interplay,

$$A(1,2,\ldots,6|\ell) = A_{\rm box}(1,2,\ldots,6) + A_{\rm pent}(1,2,\ldots,6|\ell) + A_{\rm hex}(1,2,\ldots,6|\ell) \ . \tag{4.19}$$

The highest power of loop momentum in the numerators of $A_{\rm pent}(\ldots)$ and $A_{\rm hex}(\ldots)$ is one and two, respectively.

4.4.1. Six-point boxes

The 21 boxes in the cubic-graph representation of the six-point amplitude can be described by the following 15 Berends–Giele currents (4.17) and box propagators (4.9),

$$\begin{aligned} A_{\rm box}(1,2,\ldots,6) = \frac{1}{4}\Big[&\mathcal{N}^{(4)}_{123|4,5,6} I^{(4)}_{123,4,5,6} + \mathcal{N}^{(4)}_{1|234,5,6} I^{(4)}_{1,234,5,6} + \mathcal{N}^{(4)}_{1|2,345,6} I^{(4)}_{1,2,345,6} \\ &+ \mathcal{N}^{(4)}_{1|2,3,456} I^{(4)}_{1,2,3,456} + \mathcal{N}^{(4)}_{561|2,3,4} I^{(4)}_{561,2,3,4} + \mathcal{N}^{(4)}_{612|3,4,5} I^{(4)}_{612,3,4,5} \\ &+ \mathcal{N}^{(4)}_{12|34,5,6} I^{(4)}_{12,34,5,6} + \mathcal{N}^{(4)}_{12|3,45,6} I^{(4)}_{12,3,45,6} + \mathcal{N}^{(4)}_{12|3,4,56} I^{(4)}_{12,3,4,56} \\ &+ \mathcal{N}^{(4)}_{1|23,45,6} I^{(4)}_{1,23,45,6} + \mathcal{N}^{(4)}_{1|23,4,56} I^{(4)}_{1,23,4,56} + \mathcal{N}^{(4)}_{1|2,34,56} I^{(4)}_{1,2,34,56} \\ &+ \mathcal{N}^{(4)}_{61|23,4,5} I^{(4)}_{61,23,4,5} + \mathcal{N}^{(4)}_{61|2,34,5} I^{(4)}_{61,2,34,5} + \mathcal{N}^{(4)}_{61|2,3,45} I^{(4)}_{61,2,3,45}\Big] \,. \end{aligned} \tag{4.20}$$

Given the universal form of box numerators (4.12) and their Berends–Giele currents (4.17), the superfield and pole content of any term in (4.20) can be straightforwardly recovered. For example, locality is evident from

$$\begin{aligned} \mathcal{N}^{(4)}_{123|4,5,6} I^{(4)}_{123,4,5,6} &= \left(\frac{V_{123}}{s_{12}s_{123}} + \frac{V_{321}}{s_{23}s_{123}}\right) \frac{T_{4,5,6}}{\ell^2(\ell-k_{123})^2(\ell-k_{1234})^2(\ell-k_{12345})^2} \\ \mathcal{N}^{(4)}_{12|34,5,6} I^{(4)}_{12,34,5,6} &= \frac{V_{12}T_{34,5,6}}{s_{12}s_{34}\ell^2(\ell-k_{12})^2(\ell-k_{1234})^2(\ell-k_{12345})^2} \,. \end{aligned} \tag{4.21}$$

The BRST variation of the boxes is most conveniently expressed in terms of

$$M_{12} \equiv \frac{V_{12}}{s_{12}} \,, \quad M_{23,4,5} \equiv \frac{T_{23,4,5}}{s_{23}} \,, \quad M_1 \equiv V_1 \,, \quad M_{2,3,4} \equiv T_{2,3,4} \tag{4.22}$$

and given by

$$\begin{aligned} 4Q A_{\rm box}(1,2,\ldots,6) = &\\ &M_1M_2M_{34,5,6}\big(I^{(4)}_{12,34,5,6} - I^{(4)}_{1,234,5,6}\big) + M_1M_2M_{45,3,6}\big(I^{(4)}_{12,3,45,6} - I^{(4)}_{1,23,45,6}\big) \\ &+ M_1M_2M_{56,3,4}\big(I^{(4)}_{12,3,4,56} - I^{(4)}_{1,23,4,56}\big) + M_1M_3M_{45,2,6}\big(I^{(4)}_{1,23,45,6} - I^{(4)}_{1,2,345,6}\big) \\ &+ M_1M_3M_{56,2,4}\big(I^{(4)}_{1,23,4,56} - I^{(4)}_{1,2,34,56}\big) + M_1M_4M_{23,5,6}\big(I^{(4)}_{1,234,5,6} - I^{(4)}_{1,23,45,6}\big) \\ &+ M_1M_4M_{56,2,3}\big(I^{(4)}_{1,2,34,56} - I^{(4)}_{1,2,3,456}\big) + M_1M_5M_{23,4,6}\big(I^{(4)}_{1,23,45,6} - I^{(4)}_{1,23,4,56}\big) \\ &+ M_1M_5M_{34,2,6}\big(I^{(4)}_{1,2,345,6} - I^{(4)}_{1,2,34,56}\big) + M_1M_6M_{23,4,5}\big(I^{(4)}_{1,23,4,56} - I^{(4)}_{61,23,4,5}\big) \\ &+ M_1M_6M_{34,2,5}\big(I^{(4)}_{1,2,34,56} - I^{(4)}_{61,2,34,5}\big) + M_1M_6M_{45,2,3}\big(I^{(4)}_{1,2,3,456} - I^{(4)}_{61,2,3,45}\big) \\ &+ M_1M_{23}M_{4,5,6}\big(I^{(4)}_{123,4,5,6} - I^{(4)}_{1,234,5,6}\big) + M_1M_{34}M_{2,5,6}\big(I^{(4)}_{1,234,5,6} - I^{(4)}_{1,2,345,6}\big) \\ &+ M_1M_{45}M_{2,3,6}\big(I^{(4)}_{1,2,345,6} - I^{(4)}_{1,2,3,456}\big) + M_1M_{56}M_{2,3,4}\big(I^{(4)}_{1,2,3,456} - I^{(4)}_{561,2,3,4}\big) \\ &+ M_2M_{16}M_{3,4,5}\big(I^{(4)}_{612,3,4,5} - I^{(4)}_{61,23,4,5}\big) + M_3M_{12}M_{4,5,6}\big(I^{(4)}_{12,34,5,6} - I^{(4)}_{123,4,5,6}\big) \\ &+ M_3M_{16}M_{2,4,5}\big(I^{(4)}_{61,23,4,5} - I^{(4)}_{61,2,34,5}\big) + M_4M_{12}M_{3,5,6}\big(I^{(4)}_{12,3,45,6} - I^{(4)}_{12,34,5,6}\big) \\ &+ M_4M_{16}M_{2,3,5}\big(I^{(4)}_{61,2,34,5} - I^{(4)}_{61,2,3,45}\big) + M_5M_{12}M_{3,4,6}\big(I^{(4)}_{12,3,4,56} - I^{(4)}_{12,3,45,6}\big) \\ &+ M_5M_{16}M_{2,3,4}\big(I^{(4)}_{61,2,3,45} - I^{(4)}_{561,2,3,4}\big) + M_6M_{12}M_{3,4,5}\big(I^{(4)}_{612,3,4,5} - I^{(4)}_{12,3,4,56}\big) \,. \end{aligned} \tag{4.23}$$

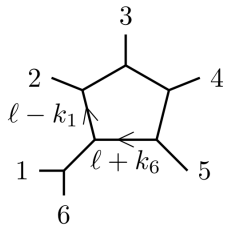

Fig. 7 Diagrammatic justification for the shift of loop momentum in $N^{(5)}_{61|2,3,4,5}(\ell+k_6)$: The shifted momentum $\ell + k_6$ occurs in the pentagon edge adjacent to the tree-level subdiagram subtending particles 6 and 1.

We will next see how this BRST variation of the boxes is cancelled by pentagons.

4.4.2. Six-point pentagons

The pentagon content of the six-point one-loop integrand is given by

$$\begin{aligned} A_{\rm pent}(1,2,\ldots,6|\ell) \equiv \frac{1}{2}\Big[&\mathcal{N}^{(5)}_{12|3,4,5,6}(\ell) I^{(5)}_{12,3,4,5,6} + \mathcal{N}^{(5)}_{1|23,4,5,6}(\ell) I^{(5)}_{1,23,4,5,6} \\ &+ \mathcal{N}^{(5)}_{1|2,34,5,6}(\ell) I^{(5)}_{1,2,34,5,6} + \mathcal{N}^{(5)}_{1|2,3,45,6}(\ell) I^{(5)}_{1,2,3,45,6} + \mathcal{N}^{(5)}_{1|2,3,4,56}(\ell) I^{(5)}_{1,2,3,4,56} \\ &+ I^{(5)}_{61,2,3,4,5}\left(\mathcal{N}^{(5)}_{61|2,3,4,5}(\ell+k_6) - V_1 J_{6|2,3,4,5}\right)\Big] \ . \end{aligned} \tag{4.24}$$

The new building block $J_{6|2,3,4,5}$ will be defined below, and the first five numerators follow the universal form (4.14) of pentagons such as

$$\begin{aligned} \mathcal{N}^{(5)}_{12|3,4,5,6}(\ell) = \frac{1}{s_{12}}\Big\{&\ell_m V_{12} T^m_{3,4,5,6} + \frac{1}{2}\big[V_{123} T_{4,5,6} + (3 \leftrightarrow 4,5,6)\big] \\ &+ \frac{1}{2}\big[V_{12} T_{34,5,6} + (3,4|3,4,5,6)\big]\Big\} \ . \end{aligned} \tag{4.25}$$

The tree-level propagator stems from (4.16), and we identify $V_{123} \equiv V_{[12,3]}$. It is easy to check from (2.8), (3.11) and (3.12) that the BRST variation of (4.25) cancels propagators,

$$\begin{aligned} Q\mathcal{N}^{(5)}_{12|3,4,5,6}(\ell) = &-V_2 N^{(5)}_{1|3,4,5,6}(\ell) + \frac{1}{2} V_1 (V_{23} T_{4,5,6} + V_{24} T_{3,5,6} + V_{25} T_{3,4,6} + V_{26} T_{3,4,5}) \\ &- M_{12} M_3 M_{4,5,6} \frac{1}{2}\big[(\ell - k_{12})^2 - (\ell - k_{123})^2\big] - M_{12} M_4 M_{3,5,6} \frac{1}{2}\big[(\ell - k_{123})^2 - (\ell - k_{1234})^2\big] \\ &- M_{12} M_5 M_{3,4,6} \frac{1}{2}\big[(\ell - k_{1234})^2 - (\ell - k_{12345})^2\big] - M_{12} M_6 M_{3,4,5} \frac{1}{2}\big[(\ell - k_{12345})^2 - \ell^2\big] \ , \end{aligned} \tag{4.26}$$

in lines with (3.16).

The last pentagon in (4.24) requires further explanation since its numerator deviates from the naive expectation $N^{(5)}_{61|2,3,4,5}(\ell)$ by $-V_{16} k^6_m T^m_{2,3,4,5} - V_1 s_{16} J_{6|2,3,4,5}$ with

$$J_{6|2,3,4,5} \equiv \frac{1}{2} A^6_m (T^m_{2,3,4,5} + W^m_{2,3,4,5}) \ . \tag{4.27}$$

The first extra term can be absorbed into a redefinition of the loop momentum to yield $N^{(5)}_{61|2,3,4,5}(\ell+k_6)-V_1 s_{16} J_{6|2,3,4,5}$. As visualized in fig. 7, the effective loop momentum $\ell+k_6$ is determined by the pentagon edge adjacent to the cubic tree subdiagram represented by V_{61}. The second extra term $\sim J_{6|2,3,4,5}$ contributes to the hexagon anomaly via[6]

$$QJ_{6|2,3,4,5} \equiv Y_{2,3,4,5,6} + V_6 k_m^6 T^m_{2,3,4,5} + \big[V_{62}T_{3,4,5} + (2 \leftrightarrow 3,4,5)\big] \,, \tag{4.28}$$

with anomaly superfield $Y_{2,3,4,5,6}$ defined in (3.13). Together with the shift of loop momentum $\sim V_{16}k_m^6 T^m_{2,3,4,5}$, the variation (4.28) ensures that the overall pentagon numerator satisfies the criterion (3.16),

$$\begin{aligned} &Q\big[\mathcal{N}^{(5)}_{61|2,3,4,5}(\ell+k_6) - V_1 J_{6|2,3,4,5}\big] = V_6 N^{(5)}_{1|2,3,4,5}(\ell) \\ &+\frac{1}{2}V_1(V_{62}T_{3,4,5}+V_{63}T_{2,4,5}+V_{64}T_{2,3,5}+V_{65}T_{2,3,4}) + M_{16}M_2M_{3,4,5}\frac{1}{2}\big[(\ell-k_1)^2-(\ell-k_{12})^2\big] \\ &+ M_{16}M_3M_{2,4,5}\frac{1}{2}\big[(\ell-k_{12})^2-(\ell-k_{123})^2\big] + M_{16}M_4M_{2,3,5}\frac{1}{2}\big[(\ell-k_{123})^2-(\ell-k_{1234})^2\big] \\ &+ M_{16}M_5M_{2,3,4}\frac{1}{2}\big[(\ell-k_{1234})^2-(\ell-k_{12345})^2\big] \,, \end{aligned} \tag{4.29}$$

which would be violated by the naive choice $N^{(5)}_{61|2,3,4,5}(\ell)$. Generally speaking, the choice of loop momentum (4.8) requires redefinitions in any $(n \geq 5)$-gon numerator where an external tree involves particles $\ldots n1\ldots$ and thereby removes the ℓ^2 propagator. The superfield $J_{6|2,3,4,5}$ can be viewed as the BRST completion of the shift of loop momentum.

The BRST variation of the remaining pentagons takes a form similar to (4.26) and (4.29). This compensates for the BRST variation (4.23) of the boxes by cancellation of propagators such as

$$(\ell-k_{12})^2 I^{(5)}_{12,3,4,5,6} = I^{(4)}_{123,4,5,6}, \quad (\ell-k_{123})^2 I^{(5)}_{12,3,4,5,6} = I^{(4)}_{12,34,5,6}\,. \tag{4.30}$$

By adding up the contributions of all box and pentagon diagrams, we find

$$4QA_{\text{pent}}(1,2,3,4,5,6|\ell) = -4QA_{\text{box}}(1,2,3,4,5,6) \tag{4.31}$$

[6] This identity was firstly noticed in [29] to express the contractions of $V_6 T^m_{2,3,4,5}$ with external momenta in terms of scalar building blocks. In the five-point context of this reference, the anomalous contribution $Y_{2,3,4,5,6}$ drops out by momentum conservation.

$$
\begin{aligned}
&+2V_1Y_{2,3,4,5,6}I^{(5)}_{61,2,3,4,5}+2V_2N^{(5)}_{1|3,4,5,6}(\ell)\big[I^{(5)}_{1,23,4,5,6}-I^{(5)}_{12,3,4,5,6}\big]\\
&+2V_3N^{(5)}_{1|2,4,5,6}(\ell)\big[I^{(5)}_{1,2,34,5,6}-I^{(5)}_{1,23,4,5,6}\big]+2V_4N^{(5)}_{1|2,3,5,6}(\ell)\big[I^{(5)}_{1,2,3,45,6}-I^{(5)}_{1,2,34,5,6}\big]\\
&+2V_5N^{(5)}_{1|2,3,4,6}(\ell)\big[I^{(5)}_{1,2,3,4,56}-I^{(5)}_{1,2,3,45,6}\big]+2V_6N^{(5)}_{1|2,3,4,5}(\ell)\big[I^{(5)}_{61,2,3,4,5}-I^{(5)}_{1,2,3,4,56}\big]\\
&+V_1V_{23}T_{4,5,6}\big[I^{(5)}_{12,3,4,5,6}-I^{(5)}_{1,2,34,5,6}\big]+V_1V_{34}T_{2,5,6}\big[I^{(5)}_{1,23,4,5,6}-I^{(5)}_{1,2,3,45,6}\big]\\
&+V_1V_{45}T_{2,3,6}\big[I^{(5)}_{1,2,34,5,6}-I^{(5)}_{1,2,3,4,56}\big]+V_1V_{56}T_{2,3,4}\big[I^{(5)}_{1,2,3,4,56}-I^{(5)}_{61,2,3,4,5}\big]\\
&+V_1V_{24}T_{3,5,6}\big[I^{(5)}_{12,3,4,5,6}-I^{(5)}_{1,23,4,5,6}+I^{(5)}_{1,2,34,5,6}-I^{(5)}_{1,2,3,45,6}\big]\\
&+V_1V_{25}T_{3,4,6}\big[I^{(5)}_{12,3,4,5,6}-I^{(5)}_{1,23,4,5,6}+I^{(5)}_{1,2,3,45,6}-I^{(5)}_{1,2,3,4,56}\big]\\
&+V_1V_{26}T_{3,4,5}\big[I^{(5)}_{12,3,4,5,6}-I^{(5)}_{1,23,4,5,6}+I^{(5)}_{1,2,3,4,56}-I^{(5)}_{61,2,3,4,5}\big]\\
&+V_1V_{35}T_{2,4,6}\big[I^{(5)}_{1,23,4,5,6}-I^{(5)}_{1,2,34,5,6}+I^{(5)}_{1,2,3,45,6}-I^{(5)}_{1,2,3,4,56}\big]\\
&+V_1V_{36}T_{2,4,5}\big[I^{(5)}_{1,23,4,5,6}-I^{(5)}_{1,2,34,5,6}+I^{(5)}_{1,2,3,4,56}-I^{(5)}_{61,2,3,4,5}\big]\\
&+V_1V_{46}T_{2,3,5}\big[I^{(5)}_{1,2,34,5,6}-I^{(5)}_{1,2,3,45,6}+I^{(5)}_{1,2,3,4,56}-I^{(5)}_{61,2,3,4,5}\big]\,.
\end{aligned}
$$

As mentioned before, the above terms beyond the first line come from cancellations of external tree propagators and must be cancelled by the BRST variation of the hexagon.

4.4.3. Six-point hexagon

The six-point hexagon whose BRST variation cancels the terms in (4.31) is given by,

$$
A_{\rm hex}(1,2,3,4,5,6|\ell)=I^{(6)}_{1,2,3,4,5,6}\,N^{(6)}_{1|2,3,4,5,6}(\ell)\,, \tag{4.32}
$$

where $N^{(6)}_{1|2,3,4,5,6}(\ell)=n^{(6)}_{1|2,3,4,5,6}(\ell)+n^{(6)}_{1|2,3,4,5,6}$ and all the ℓ-dependent part of the local hexagon numerator is represented by

$$
\begin{aligned}
n^{(6)}_{1|2,3,4,5,6}(\ell)=\frac{1}{2}\ell_m\ell_nV_1T^{mn}_{2,3,4,5,6}+\frac{1}{2}\ell_m\big[V_{12}T^m_{3,4,5,6}+(2\leftrightarrow 3,4,5,6)\big]\\
+\frac{1}{2}\ell_mV_1\big[T^m_{23,4,5,6}+(2,3|2,3,4,5,6)\big]\,.
\end{aligned} \tag{4.33}
$$

This is analogous to the five-point pentagon (4.5) with building blocks of higher ranks and another contraction with ℓ_m. Note that the tensor building block $T^{mn}_{2,3,4,5,6}$ defined in (3.9) introduces an anomalous contribution $\sim Y_{2,3,4,5,6}$ to the BRST variation due to (3.12).

The scalar hexagon, on the other hand, is determined by (3.16): The Q variation of (4.32) must be expressible in terms of hexagon propagators $(\ell-k_{12\ldots j})^2$ with $j=0,1,\ldots,5$.

Apart from $Y_{2,3,4,5,6}$, this is only possible if any factor of $(\ell \cdot k_j)$ in the variation of (4.33) is accompanied by $-(s_{1j} + s_{2j} + \ldots + s_{j-1,j})$ to build up the difference

$$(\ell - k_{12\ldots j})^2 - (\ell - k_{12\ldots j-1})^2 = -2(\ell \cdot k_j) + 2(s_{1j} + s_{2j} + \ldots + s_{j-1,j}) \ . \tag{4.34}$$

The unique local superfield which is compatible with this requirement and constructed out of the building blocks in section 2.3 reads

$$\begin{aligned} n^{(6)}_{1|2,3,4,5,6} &= \frac{1}{4}\big[V_1 T_{23,45,6} + (2,3|4,5|2,3,4,5,6)\big] + \frac{1}{4}\big[V_{12} T_{34,5,6} + (2|3,4|2,3,4,5,6)\big] \\ &+ \frac{1}{6}\big[(V_1 T_{234,5,6} + V_1 T_{432,5,6}) + (2,3,4|2,3,4,5,6)\big] - \frac{1}{12}\big[(k^1_m - k^2_m) V_{12} T^m_{3,4,5,6} + (2 \leftrightarrow 3,4,5,6)\big] \\ &+ \frac{1}{6}\big[(V_{123} T_{4,5,6} + V_{321} T_{4,5,6}) + (2,3|2,3,4,5,6)\big] - \frac{1}{12}\big[(k^2_m - k^3_m) V_1 T^m_{23,4,5,6} + (2,3|2,3,4,5,6)\big] \\ &- \frac{1}{24} V_1 T^{mn}_{2,3,4,5,6}\big[k^1_m k^1_n + (1 \leftrightarrow 2,3,4,5,6)\big] \ . \end{aligned} \tag{4.35}$$

The notation $(2,3|4,5|2,3,4,5,6)$ instructs to sum all possible ways to distribute the set of labels $\{2,3,\ldots,6\}$ into two *ordered* sets $\{2,3\}$ and $\{4,5\}$ without double counting where the ordering is with respect to the set $\{2,3,\ldots,6\}$. For example, $\{2,4\},\{5,3\}$ is not an allowed distribution because it violates the ordering in the second set, and only one of $\{2,5\},\{3,6\}$ and $\{3,6\},\{2,5\}$ enters (4.35) to avoid overcounting. A similar convention holds for $(2|3,4|2,3,4,5,6)$.

A long but straightforward analysis shows that the hexagon (4.32) has the required properties to make the whole six-point one-loop integrand (4.19) (naively) BRST invariant,

$$QA(1,2,\ldots,6|\ell) = \frac{1}{2} V_1 Y_{2,3,4,5,6} (I^{(5)}_{61,2,3,4,5} - \ell^2 I^{(6)}_{1,2,3,4,5,6}) \, . \tag{4.36}$$

The right-hand side keeps track of the anomalous contributions due to the tensor hexagon $Q\frac{1}{2}\ell_m \ell_n V_1 T^{mn}_{2,3,4,5,6}$ and the second line of the pentagon variation in (4.31). By inserting the propagators in (4.11) and $I^{(6)}_{1,2,3,4,5,6} = \prod_{j=0}^5 (\ell - k_{12\ldots j})^{-2}$, the variation (4.36) appears to cancel at the level of the integrand. However, the logarithmically divergent nature of the ten-dimensional integral over (4.36) leads to subtleties to be resolved in the subsequent.

4.5. The gauge anomaly of the six-point amplitude

In this subsection, we perform a worldline analysis of the anomalous BRST variation (4.36) of the one-loop SYM six point amplitude. The string-based formalism gives rise to

the following worldline representation of a N-gon integral in D dimensions [30]

$$\int \frac{d^D\ell\ (p+q_m\ell^m+r_{mn}\ell^m\ell^n)}{\ell^2(\ell-k_1)^2(\ell-k_{12})^2\ldots(\ell-k_{12\ldots N-1})^2} = \int d^D\ell\ I^{(N)}_{1,2,\ldots,N}(p+q_m\ell^m+r_{mn}\ell^m\ell^n) \quad (4.37)$$
$$= \pi^N\int_0^\infty \frac{dt}{t}\,t^{N-\frac{D}{2}} \int\limits_{0\leq\nu_i\leq\nu_{i+1}\leq 1} d\nu_2\,d\nu_3\,\ldots\,d\nu_n\,\Big(p+q_mL^m+r_{mn}\Big[L^mL^n+\frac{\delta^{mn}}{2\pi t}\Big]\Big)e^{-\pi tQ_N}\,\Big|_{\nu_1=0}$$

where p, q_m and r_{mn} are arbitrary scalars, vectors and tensors independent on ℓ. We use the following shorthands for the shift in loop momentum L^m and the exponent Q_N,

$$L^m \equiv -\sum_{i=1}^N k_i^m\nu_i\ , \qquad Q_N \equiv \sum_{1\leq i<j}^N s_{ij}(\nu_{ij}^2-|\nu_{ij}|)\ , \quad (4.38)$$

where $\nu_{ij}\equiv\nu_i-\nu_j$ and $\nu_1=0$ is implicit from now on. To make contact with the six-point anomaly, consider the following boundary term in $D=10$ dimensions,

$$B_6 \equiv -\pi^5\int_0^\infty dt\ \frac{\partial}{\partial t}\Big\{t^{5-\frac{D}{2}}\int\limits_{0\leq\nu_i\leq\nu_{i+1}\leq 1} d\nu_2\,d\nu_3\,\ldots\,d\nu_6\,e^{-\pi tQ_6}\Big\}\Big|_{D=10} = \frac{\pi^5}{5!}\ , \quad (4.39)$$

which yields the volume of a five-simplex from the lower integration limit $t=0$. For hexagons at $N=6$, the exponential in (4.37) satisfies the differential equation

$$-\frac{1}{\pi}\,\frac{\partial}{\partial t}e^{-\pi tQ_6} = \Big(L_mL^m+\frac{5}{\pi t}\Big)e^{-\pi tQ_6}+\frac{1}{\pi t}\sum_{p=2}^6(\partial_{\nu_p}\nu_{1p}e^{-\pi tQ_6})\ , \quad (4.40)$$

which allows for the following rewriting of the boundary term B_6:

$$B_6 = \pi^6\int_0^\infty dt\ t^{5-D/2}\int\limits_{0\leq\nu_i\leq\nu_{i+1}\leq 1} d\nu_2\ \ldots\ d\nu_6\,\Big\{L^2+\frac{5}{\pi t}+\frac{1}{\pi t}\sum_{p=2}^n\partial_{\nu_p}\nu_{1p}\Big\}\,e^{-\pi tQ_6}\ . \quad (4.41)$$

The ∂_{ν_p} derivatives in the last term are understood to also act on $e^{-\pi tQ_6}$. They can be evaluated as a series of boundary terms $\nu_i\to\nu_{i\pm1}$ with $\nu_1=0$ and $\nu_7=1$ where only the upper limit of the ν_6 integration remains uncancelled. With $\nu_{17}=-1$, the result is

$$B_6 = \pi^6\int_0^\infty dt\ t^{5-D/2}\int\limits_{0\leq\nu_i\leq\nu_{i+1}<1} d\nu_2\ \ldots\ d\nu_6\,\Big\{L^2+\frac{5}{\pi t}-\frac{\delta(\nu_6-1)}{\pi t}\Big\}\,e^{-\pi tQ_6}\ . \quad (4.42)$$

The first two terms can be recognized as a tensor hexagon with $r_{mn}=\delta_{mn}$, see (4.37) at $N=6,\ D=10$ and $p=q_m=0$. The last term, on the other hand, describes a scalar pentagon, hence we recover both integrals in the anomalous BRST variation (4.36):

$$B_6 = \int d^D\ell\,\big(\ell^2I^{(6)}_{1,2,3,4,5,6}-I^{(5)}_{61,2,3,4,5}\big) \quad (4.43)$$

Using the value of B_6 found in (4.39), the BRST variation of the six point amplitude turns out to be a rational function in external momenta,

$$Q\int d^D\ell\, A(1,2,3,4,5,6|\ell) = -\frac{1}{2}V_1 Y_{2,3,4,5,6} B_6 = -\frac{\pi^5}{240}V_1 Y_{2,3,4,5,6}\ . \tag{4.44}$$

Note that the BRST anomaly $QA(1,2,3,4,5,6|\ell) \sim V_1 Y_{2,3,4,5,6}$ is equivalent to the anomalous gauge variation $\delta_1 A(1,2,3,4,5,6|\ell) \sim \langle \Omega_1 Y_{2,3,4,5,6}\rangle$, see the appendix of [16], in lines with the anomaly analysis of the pure spinor superstring [26]. Gauge variations in pure spinor superspace amount to insertions of a BRST-exact vertex $\delta_1 V_1 = Q\Omega_1$ with some scalar superfield Ω_1.

The discussion of [31] is helpful to shed further light on the apparent paradox between the formally vanishing integrand in (4.43) and the finite result in (4.39): In a dimensional regularization scheme $D \to D - 2\varepsilon$, anomalies in chiral gauge theories arise from components of the loop momentum in the fractional -2ε dimensions. The idea is to formally split the $D-2\varepsilon$ dimensional loop momentum into $\ell^2_{D-2\varepsilon} = \ell^2_D + \mu^2$ with D dimensional part ℓ_D and "-2ε dimensional" component μ. The tensor hexagon numerator along with $I^{(6)}_{1,2,3,4,5,6}$ remains $\ell^m_D \ell^n_D$ in $D-2\varepsilon$ dimensions since the loop momenta are contracted into the D dimensional polarization tensors from the *external* states in $T^{mn}_{2,3,4,5,6}$. The *internal* states propagating through the loop, however, give rise to momenta $\ell_{D-2\varepsilon}$ in the propagators, so the integrand (4.36) is proportional to $\ell^2_D - \ell^2_{D-2\varepsilon} = -\mu^2$.

This argument based on dimensional regularization also explains why none of the other cancellations among ℓ-dependent propagators in $QA(1,2,\ldots,n|\ell)$ introduces rational terms: Since $(\ell_D{\cdot}k_j) = (\ell_{D-2\varepsilon}{\cdot}k_j)$ for D-dimensional external momenta, we can still rewrite

$$(\ell_D \cdot k_j) = \frac{1}{2}\big[(\ell_{D-2\varepsilon} - k_{12\ldots j-1})^2 - (\ell_{D-2\varepsilon} - k_{12\ldots j})^2\big] + s_{1j} + s_{2j} + \ldots + s_{j-1,j} \tag{4.45}$$

and cancel propagators with $(D-2\varepsilon)$-dimensional loop momenta on the right-hand side.

5. Manifestly BRST pseudo-invariant SYM integrands

In this section, we manifest the BRST- and cyclicity properties of the above SYM integrands by rewriting the kinematic numerators in terms of (almost) BRST invariant superfields where only the fingerprints of the hexagon anomaly appear in the Q variation.

5.1. Manifesting BRST pseudo-invariance

The above cohomology construction of the six-point amplitude suggests that anomalous superfields such as $Y_{A,B,C,D,E}$ in (3.13) have to be treated separately in the analysis of BRST properties. This led to call a superfield *BRST-pseudo-invariant* if each term in its BRST variation contains an anomalous factor of $Y_{A,B,C,D,E}$ [16].

A procedure is described in [16] to recursively construct BRST pseudo-invariants from superfields $V_A T^{mn\ldots}_{B_1,B_2,B_3,\ldots}$ as defined in section 3.2. The setup in [16] also includes $J_{1|2,3,4,5}$ in (4.27) as well as generalizations to arbitrary rank and multiplicity. These pseudo-invariant are denoted by $C^{mn\ldots}_{1|B_1,B_2,\ldots}$ or $P_{1|6|2,3,4,5}$ and classified by a term $V_1 T^{mn\ldots}_{B_1,B_2,B_3,\ldots}$ or $V_1 J_{6|2,3,4,5}$ with a single particle representative V_1 of the unintegrated vertex. The pseudo-invariant completion of these terms is furnished by multiparticle versions of $V_{12\ldots p}$ with $p \geq 2$ and most conveniently described in the basis of Berends–Giele currents such as (4.22). Similar to $T^{mn\ldots}_{B_1,B_2,B_3,\ldots}$ and $J_{6|2,3,4,5}$, the pseudo-invariants $C^{mn\ldots}_{1|B_1,B_2,\ldots}$ and $P_{1|6|2,3,4,5}$ are symmetric under exchange of slots B_j which are separated by a comma.

At $n \leq 5$ points, for instance, it is straightforward to show that

$$\begin{aligned} C_{1|2,3,4} &\equiv M_1 M_{2,3,4} \\ C_{1|23,4,5} &\equiv M_1 M_{23,4,5} + M_{12} M_{3,4,5} - M_{13} M_{2,4,5} \\ C^m_{1|2,3,4,5} &\equiv M_1 T^m_{2,3,4,5} + \big[k_2^m M_{12} M_{3,4,5} + (2 \leftrightarrow 3,4,5)\big] \end{aligned} \tag{5.1}$$

are BRST closed. For the six-point BRST invariants $C_{1|234,5,6}, C_{1|23,45,6}$ and $C^m_{1|23,4,5,6}$, analogous superfield expansions can be found in [12,16]. Reference [16] also displays the first pseudo-invariants $C^{mn}_{1|2,3,4,5,6}$ as well as

$$P_{1|6|2,3,4,5} \equiv V_1 J_{6|2,3,4,5} + M_{16} k_m^6 T^m_{2,3,4,5} + \big[M_{162} T_{3,4,5} + (2 \leftrightarrow 3,4,5)\big] \tag{5.2}$$

with $M_{123} = \frac{1}{s_{123}}(\frac{V_{123}}{s_{12}} + \frac{V_{321}}{s_{23}})$ subject to

$$QC^{mn}_{1|2,3,4,5,6} = -\delta^{mn} V_1 Y_{2,3,4,5,6} \ , \qquad QP_{1|6|2,3,4,5} = -V_1 Y_{2,3,4,5,6} \ . \tag{5.3}$$

For external gluons, the explicit component expansions can be downloaded from [19]. Note that any scalar invariant $C_{1|A,B,C}$ can be expanded in terms of SYM tree amplitudes using the general formula given in the appendix of [12], see the five-point examples below.

As experimentally observed in [16], one can rewrite BRST pseudo-invariant expressions in terms of manifestly BRST pseudo-invariant building blocks by mapping

$$\begin{aligned}
&V_{12\ldots p}\big|_{p\geq 2} \to 0 \ , \quad V_1 T_{23,4,5} \to s_{23} C_{1|23,4,5} \ , \quad V_1 T^m_{2,3,4,5} \to C^m_{1|2,3,4,5} \\
&V_1 T_{234,5,6} \to s_{23}(s_{34} C_{1|234,5,6} - s_{24} C_{1|324,5,6}) \ , \quad V_1 T_{23,45,6} \to s_{23} s_{45} C_{1|23,45,6} \\
&V_1 T^m_{23,4,5,6} \to s_{23} C^m_{1|23,4,5,6} \ , \quad V_1 T^{mn}_{2,3,4,5,6} \to C^{mn}_{1|2,3,4,5,6} \ , \quad V_1 J_{6|2,3,4,5} \to P_{1|6|2,3,4,5} \ .
\end{aligned} \tag{5.4}$$

Any appearance of V_1 signals a pseudo-invariant, whereas the multiparticle instances of $V_{12\ldots p}$ with $p \geq 2$ are absorbed into the BRST completion of the former. When manifesting BRST pseudo-invariance of the superspace integrand $A(1,2,\ldots,n|\ell)$ at $n = 5, 6$, the prescription (5.4) allows to foresee the result of algebraic manipulations among the (possibly ℓ dependent) propagators. However, the different kinematic poles in the expressions (5.1) for $C_{1|23,4,5}$ and $C^m_{1|2,3,4,5}$ exemplify that locality is obscured when the five-point amplitude is expressed in terms of BRST invariants. Hence, the representations for $A(1,2,\ldots,n|\ell)$ discussed in the subsequent trade manifest locality for manifest BRST pseudo-invariance.

5.2. Five-point one-loop integrand

Applying the map in (5.4) to the five-point integrand (4.2) and writing down the explicit integrands leads to

$$\begin{aligned}
A(1,2,3,4,5|\ell) = &\frac{\frac{1}{2} C_{1|23,4,5}}{\ell^2(\ell-k_1)^2(\ell-k_{123})^2(\ell-k_{1234})^2} + \frac{\frac{1}{2} C_{1|34,2,5}}{\ell^2(\ell-k_1)^2(\ell-k_{12})^2(\ell-k_{1234})^2} \\
&+ \frac{\frac{1}{2} C_{1|45,2,3}}{\ell^2(\ell-k_1)^2(\ell-k_{12})^2(\ell-k_{123})^2} + \frac{C_{1|2;3;4;5} + \ell_m C^m_{1|2,3,4,5}}{\ell^2(\ell-k_1)^2(\ell-k_{12})^2(\ell-k_{123})^2(\ell-k_{1234})^2} \ ,
\end{aligned} \tag{5.5}$$

see (5.1) for $C_{1|23,4,5}$ and $C^m_{1|2,3,4,5}$. The scalar pentagon is represented by the shorthand

$$C_{1|2;3;4;5} = \frac{1}{2}\big[s_{23} C_{1|23,4,5} + (2,3|2,3,4,5)\big] \tag{5.6}$$

and can be obtained from $N_{1|2,3,4,5}(\ell = 0)$ under (5.4). Using the expansion of the invariants given in (5.1), it is a matter of algebraic manipulations to check that (5.5) agrees with the local representation in section 4.2 at the level of the integrand. For example, the massive box $I^{(4)}_{12,3,4,5}$ can be eliminated using

$$I^{(4)}_{12,3,4,5} = I^{(4)}_{1,23,4,5} + 2 I^{(5)}_{1,2,3,4,5}\big[(\ell \cdot k_2) - s_{12}\big] \ . \tag{5.7}$$

The scalar invariants in (5.5) are related to SYM tree subamplitudes through

$$\begin{aligned}\langle C_{1|23,4,5}\rangle &= s_{45}\big[s_{24}A^{\rm tree}(1,3,2,4,5) - s_{34}A^{\rm tree}(1,2,3,4,5)\big]\\ \langle C_{1|2;3;4;5}\rangle &= \frac{s_{23}s_{45}}{s_{14}}\big[s_{12}s_{34}\,A^{\rm tree}(1,2,3,4,5) - s_{24}(s_{12}+s_{15})A^{\rm tree}(1,3,2,4,5)\big]\ ,\end{aligned} \tag{5.8}$$

and integrals over $\ell^m C^m_{1|2,3,4,5}$ boil down to permutations of

$$\langle k_m^4 C^m_{1|2,3,4,5}\rangle = -s_{24}s_{34}s_{45}\big[A^{\rm tree}(1,2,3,4,5) + A^{\rm tree}(1,3,2,4,5)\big]\ , \tag{5.9}$$

see (A.4) for the Schwinger parametrizaton of the vector integral. These reductions to trees furnish the five-point generalization of $\langle C_{1|2,3,4}\rangle = s_{12}s_{23}A^{\rm tree}(1,2,3,4)$ relevant for (3.1).

5.3. Six-point one-loop integrand

Similarly, applying the map (5.4) to the six-point expression (4.19) yields,

$$\begin{aligned}A(1,2,\ldots,6|\ell) = \frac{1}{4}\Big[&C_{1|234,5,6}I^{(4)}_{1,234,5,6} + C_{1|2,345,6}I^{(4)}_{1,2,345,6} + C_{1|2,3,456}I^{(4)}_{1,2,3,456}\\ &+ C_{1|23,45,6}I^{(4)}_{1,23,45,6} + C_{1|23,4,56}I^{(4)}_{1,23,4,56} + C_{1|2,34,56}I^{(4)}_{1,2,34,56}\Big]\\ &+ \frac{1}{2}\Big[(C_{1|23;4;5;6}+\ell_m C^m_{1|23,4,5,6})I^{(5)}_{1,23,4,5,6} + (C_{1|2;34;5;6}+\ell_m C^m_{1|2,34,5,6})I^{(5)}_{1,2,34,5,6}\\ &+ (C_{1|2;3;45;6}+\ell_m C^m_{1|2,3,45,6})I^{(5)}_{1,2,3,45,6} + (C_{1|2;3;4;56}+\ell_m C^m_{1|2,3,4,56})I^{(5)}_{1,2,3,4,56}\Big]\\ &+ \big(C_{1|2;3;4;5;6}+\ell_m C^m_{1|2;3;4;5;6} + \frac{1}{2}\ell_m\ell_n C^{mn}_{1|2,3,4,5,6}\big)I^{(6)}_{1,2,3,4,5,6} - \frac{1}{2}P_{1|6|2,3,4,5}I^{(5)}_{61,2,3,4,5}\ .\end{aligned} \tag{5.10}$$

The pseudo-invariants $C_{1|A,B,C}, C^m_{1|A,B,C,D}, C^{mn}_{1|2,3,4,5,6}$ and $P_{1|6|2,3,4,5}$ are defined in [16] and (5.2) whereas[7] $C_{1|23;4;5;6}$ and $C^m_{1|2;3;4;5;6}$ are shorthands for subleading powers of ℓ^m:

$$\begin{aligned}C_{1|23;4;5;6} = \frac{1}{2}\Big(&s_{45}C_{1|23,45,6} + s_{46}C_{1|23,46,5} + s_{56}C_{1|23,56,4}\\ &+ \big[s_{34}C_{1|234,5,6} - s_{24}C_{1|324,5,6} + (4\leftrightarrow 5,6)\big]\Big)\end{aligned} \tag{5.11}$$

$$C^m_{1|2;3;4;5;6} = \frac{1}{2}\big(s_{23}C^m_{1|23,4,5,6} + (2,3|2,3,4,5,6)\big)\ . \tag{5.12}$$

[7] For completeness, the remaining scalar pentagons are given by

$$\begin{aligned}2C_{1|2;34;5;6} &= s_{25}C_{1|25,34,6} + s_{26}C_{1|26,34,5} + s_{56}C_{1|2,34,56}\\ &\quad + s_{23}C_{1|234,5,6} - s_{24}C_{1|243,5,6} + \big[s_{45}C_{1|2,345,6} - s_{35}C_{1|2,435,6} + (5\leftrightarrow 6)\big]\\ 2C_{1|2;3;45;6} &= s_{23}C_{1|23,45,6} + s_{26}C_{1|26,45,3} + s_{36}C_{1|2,36,45}\\ &\quad + \big[s_{24}C_{1|245,3,6} - s_{25}C_{1|254,3,6} + (2\leftrightarrow 3)\big] + s_{56}C_{1|2,3,456} - s_{46}C_{1|2,3,546}\\ 2C_{1|2;3;4;56} &= s_{23}C_{1|23,4,56} + s_{24}C_{1|24,3,56} + s_{34}C_{1|2,34,56}\\ &\quad + \big[s_{45}C_{1|2,3,456} - s_{46}C_{1|2,3,465} + (4\leftrightarrow 2,3)\big]\ .\end{aligned}$$

Moreover, the BRST version of the scalar hexagon numerator in (4.35) is given by:

$$C_{1|2;3;4;5;6} = \frac{1}{4}s_{23}s_{45}C_{1|23,45,6} + (2,3|4,5|2,3,4,5,6) \tag{5.13}$$
$$+ \frac{1}{6}\Big[s_{23}\big(s_{34}C_{1|234,5,6} - s_{24}C_{1|324,5,6}\big) + s_{43}\big(s_{32}C_{1|432,5,6} - s_{24}C_{1|342,5,6}\big) + (2,3,4|2,3,4,5,6)\Big]$$
$$+ \frac{1}{12}\Big[(k_3^m - k_2^m)s_{23}C^m_{1|23,4,5,6} + (2,3|2,3,4,5,6)\Big] - \frac{1}{24}C^{mn}_{1|2,3,4,5,6}\big[k^1_m k^1_n + (1 \leftrightarrow 2,3,4,5,6)\big] \ .$$

The expansion of the pseudo-invariants in terms of local numerators can be found in [16]. On their basis, it is a matter of algebraic relations similar to (5.7) to verify agreement between the manifestly BRST pseudo-invariant and the manifestly local representation of $A(1,2,3,4,5,6|\ell)$. In upcoming work [32], the SYM integrand (5.10) will be shown to follow in the field-theory limit of the open superstring.

Note that the anomalous BRST variation (5.3) of $C^{mn}_{1|2,3,4,5,6}$ and $P_{1|6|2,3,4,5}$ allows to reproduce the hexagon anomaly (4.36) from (5.10).

5.4. Cyclicity of the five- and six-point integrands

As another virtue of the manifestly pseudo-invariant representations (5.5) and (5.10) of $A(1,2,\ldots,n|\ell)$, their cyclicity can be analyzed in superspace. Strictly speaking, only the integrated subamplitude in (3.14) is cyclically pseudo-invariant because the hexagon anomaly turns out to obstruct cyclic symmetry of the six-point amplitude. Starting point of the cyclicity analysis is the rewriting of the n-point amplitude (3.14) as

$$A(1,2,\ldots,n) \equiv \int \frac{d^D\ell\ \hat{A}(1,2,\ldots,n|\ell)}{\ell^2(\ell-k_1)^2(\ell-k_{12})^2\ldots(\ell-k_{12\ldots n-1})^2} \tag{5.14}$$

with *stripped integrand* $\hat{A}(1,2,\ldots,n|\ell)$. Under cyclic shifts $i \to i+n \mod n$ of all the labels, the n-gon denominator in (5.14) transforms to $\ell^2(\ell-k_2)^2(\ell-k_{23})^2\ldots(\ell-k_{234n})^2$ which can be undone by change of integration variables $\ell \to \ell - k_1$. Since this is the cyclic image of the shift $\ell \to \ell - k_n$, the integrated amplitude (5.14) is cyclically invariant if the stripped integrand satisfies

$$\hat{A}(1,2,\ldots,n|\ell-k_n)\big|_{i\to i+1 \mod n} = \hat{A}(1,2,\ldots,n|\ell) \ . \tag{5.15}$$

The method is most conveniently illustrated at the five-point level. The stripped integrand

$$\hat{A}(1,2,3,4,5|\ell) = \Big\langle \frac{1}{2}(s_{23}+2s_{345})C_{1|23,4,5} + \frac{1}{2}(s_{34}+2s_{45})C_{1|34,2,5} + \frac{1}{2}s_{45}C_{1|45,2,3}$$
$$+ \frac{1}{2}s_{24}C_{1|24,3,5} + \frac{1}{2}s_{25}C_{1|25,3,4} + \frac{1}{2}s_{35}C_{1|35,2,4} + \ell_m C^m_{1|2,3,4,5} + (\ell\cdot k_3)C_{1|23,4,5} \tag{5.16}$$
$$+ (\ell\cdot k_4)(C_{1|23,4,5} + C_{1|34,2,5}) + \Big[(\ell\cdot k_5) + \frac{1}{2}\ell^2\Big](C_{1|23,4,5} + C_{1|34,2,5} + C_{1|45,2,3})\Big\rangle$$

associated with (5.5) introduces permuted invariants such as $C_{2|34,1,5}$ and $C^m_{2|3,4,5,1}$ after the cyclic shift $i \to i+1$ mod 5. They are no longer in the canonical form $C_{1|\dots}$ and $C^m_{1|\dots}$, but a procedure to restore it is described in section 11 of [16]. After discarding appropriate BRST-exact terms, the scalar invariants in (5.16) are found to transform to

$$\begin{aligned}
\langle C_{2|34,5,1}\rangle &= \langle C_{1|34,2,5} + C_{1|23,4,5} - C_{1|24,3,5}\rangle \ , \qquad \langle C_{2|31,4,5}\rangle = \langle C_{1|23,4,5}\rangle \\
\langle C_{2|35,4,1}\rangle &= \langle C_{1|35,2,4} + C_{1|23,4,5} - C_{1|25,3,4}\rangle \ , \qquad \langle C_{2|41,3,5}\rangle = \langle C_{1|24,3,5}\rangle \\
\langle C_{2|45,3,1}\rangle &= \langle C_{1|45,2,3} + C_{1|24,3,5} - C_{1|25,3,4}\rangle \ , \qquad \langle C_{2|51,3,4}\rangle = \langle C_{1|25,3,4}\rangle
\end{aligned} \tag{5.17}$$

under $i \to i+5$ mod 5, and the vector invariant is mapped to

$$\langle C^m_{2|3,4,5,1}\rangle = \langle C^m_{1|2,3,4,5} + \big[k_3^m C_{1|23,4,5} + (3 \leftrightarrow 4,5)\big]\rangle \ . \tag{5.18}$$

At six points, the relevant cyclic shifts $i \to i+6$ mod 6 such as

$$\langle P_{2|1|3,4,5,6}\rangle = \langle P_{1|2|3,4,5,6} + \mathcal{Y}_{12,3,4,5,6}\rangle \tag{5.19}$$

$$\begin{aligned}
\langle C^{mn}_{2|3,4,5,6,1}\rangle = \langle &\delta^{mn}\mathcal{Y}_{12,3,4,5,6} + C^{mn}_{1|2,3,4,5,6} + \big[2k_3^{(m}C^{n)}_{1|23,4,5,6} + (3 \leftrightarrow 4,5,6)\big] \\
&+ \big[2k_3^{(m}k_4^{n)}(C_{1|234,5,6} + C_{1|243,5,6}) + (3,4|3,4,5,6)\big]\rangle
\end{aligned} \tag{5.20}$$

can again be found in section 11 and the appendix of [16]. The anomalous superfield

$$\mathcal{Y}_{12,3,4,5,6} \equiv \frac{1}{s_{12}} Y_{12,3,4,5,6} \tag{5.21}$$

with $Y_{12,3,4,5,6}$ defined in (3.13) measures the response of the hexagon anomaly to a cyclic shift. It has parity-odd bosonic components (with gluon polarizations e_i^p) [18]

$$\langle \mathcal{Y}_{12,3,4,5,6}\rangle = -\epsilon_{p_3p_4p_5p_6q_1q_2\dots q_6} k_3^{p_3}k_4^{p_4}k_5^{p_5}k_6^{p_6}e_1^{q_1}e_2^{q_2}\cdots e_6^{q_6} \ . \tag{5.22}$$

Apart from the subtleties associated with $\mathcal{Y}_{12,3,4,5,6}$, it is straightforward to show that the stripped integrand (5.14) associated with (5.10) satisfies (5.15). The anomalous obstruction

$$\begin{aligned}
\hat{A}(1,2,3,4,5,6|\ell-k_6)\big|_{i\to i+1 \text{ mod } 6} - \hat{A}(1,2,3,4,5,6|\ell-k_6) \\
= \frac{1}{2}\langle \mathcal{Y}_{12,3,4,5,6}\rangle\big(\delta_{mn}\ell^m\ell^n - \ell^2\big)
\end{aligned} \tag{5.23}$$

integrates to a rational term as described in section 4.5, i.e. the failure of cyclic invariance is given by

$$A(2,3,4,5,6,1) - A(1,2,3,4,5,6) = \frac{1}{(2\pi)^{10}}\frac{\pi^5}{240}\langle \mathcal{Y}_{12,3,4,5,6}\rangle \ . \tag{5.24}$$

We have kept the Kronecker delta in (5.23) explicit which stems from the cyclic transformation of the tensor-pseudoinvariant (5.20). As explained at the end of section 4.5, it can be understood from dimensional reduction that the formally vanishing integrand in (5.23) integrates to the rational expression (5.24) in external momenta.

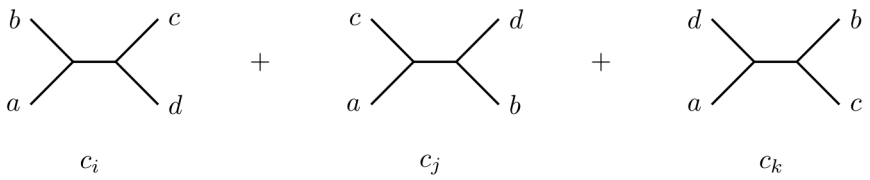

Fig. 8 The vanishing of the color factors associated to the above triplet of cubic graphs, $c_i + c_j + c_k = 0$ is a consequence of the Jacobi identity. In the above diagrams, the legs a, b, c and d may represent arbitrary subdiagrams. The BCJ duality states that their corresponding kinematic numerators N_i can be chosen such that $N_i + N_j + N_k = 0$.

6. One-loop color-kinematics duality

In 2008, Bern, Carrasco and Johansson (BCJ) proposed an organization scheme for tree-level gauge and gravity amplitudes based on cubic vertices where color and kinematics enter on completely symmetric footing [3]. Color tensors c_i are naturally associated with cubic diagrams by dressing each vertex with structure constants f^{abc} of some gauge group. Triplets of color tensors c_i, c_j, c_k associated with the diagrams shown in fig. 8 vanish due to the Jacobi identity

$$f^{abe}f^{cde} + f^{bce}f^{ade} + f^{cae}f^{bde} = 0 \tag{6.1}$$

valid for any gauge group.

The BCJ conjecture states that amplitudes can be represented such that for any vanishing color triplet $c_i + c_j + c_k$, the corresponding kinematic decorations $N_i + N_j + N_k$ of diagrams i, j, k vanish as well. The tree-level BCJ duality was later extended to loops in [28] and successfully applied to four loops [33]; also see [34] for situations with reduced supersymmetry and [35] for pure Yang-Mills and gravity. However, the vanishing triplet of kinematic numerators associated to the color triplet $c_i + c_j + c_k$ may depend on loop momenta as well, $N_i(\ell) + N_j(\ell) + N_k(\ell) = 0$. The statement that the kinematic numerators satisfy the same relations as their associated color factors is referred to as the *color-kinematic duality* or simply the *BCJ duality*.

6.1. The five-point pure spinor representation and BCJ duality

In this section the pure spinor superspace representation of the five-point one-loop amplitude will be shown to satisfy the BCJ color-kinematics duality. This generalizes the BCJ-satisfying five-point numerators given in [36] using four-dimensional spinor helicity variables to ten dimensions, see also [37].

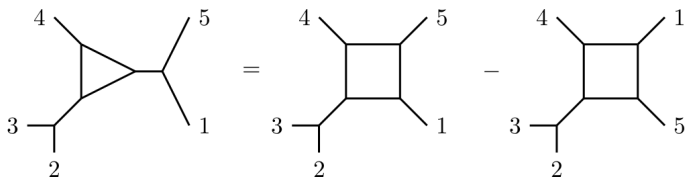

Fig. 9 Kinematic Jacobi relations relate box and triangle numerators. Since maximally SYM amplitudes are not expected to contain triangles (nor bubbles and tadpoles), the left-hand side must vanish.

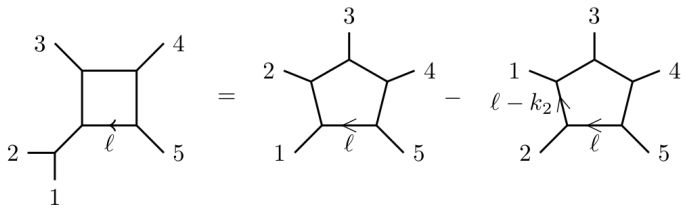

Fig. 10 Kinematic Jacobi relations relate pentagon numerators to box numerators.

6.1.1. Verifying Jacobi kinematic identities among boxes and pentagons

The BCJ identities associated to the external tree subdiagrams are trivially satisfied in the pure spinor superspace representation since they are represented by BRST blocks which manifestly satisfy the symmetries of their associated color factors[8]. In the five-point case of this subsection, this amounts to the antisymmetry of the massive legs in the boxes and is manifestly satisfied by the rank-two BRST blocks.

As discussed in [36], a representation of the five-point one-amplitude satisfies the BCJ duality if certain relations among the box and pentagon kinematic numerators hold. For example, an antisymmetrization of any two corners of a box yields a triangle numerator as shown in fig. 9. Since there are no triangles in maximally supersymmetric SYM amplitudes, this antisymmetrization of boxes must vanish if BCJ is to be obeyed. And indeed, they vanish for the pure spinor representation of section 4.2. For example, the kinematic numerators which correspond to the diagrams of the right-hand side of fig. 9 are easily seen to cancel each other,

$$\langle N^{(4)}_{1|23,4,5} - N^{(4)}_{1|5,23,4} \rangle = \langle V_1 (T_{23,4,5} - T_{5,23,4}) \rangle = 0, \tag{6.2}$$

since $T_{A,B,C}$ is symmetric in A, B, C. For any choice of massive corner in a five-point box, there is only one possible superfield assignment – either $\langle V_{12} T_{3,4,5} \rangle$ and $(2 \leftrightarrow 3, 4, 5)$ if leg

[8] For a detailed discussion of the general symmetries of BRST blocks and their compatibility with BCJ identities, see appendix A of [12].

one is part of the massive corner or $\langle V_1 T_{23,4,5}\rangle$ and $(2,3|2,3,4,5)$ otherwise. Hence, the numerators cannot contain information about the ordering of the box and every possible way to generate a triangle numerator vanishes with these superspace representatives.

There is another class of kinematic Jacobi identity that needs to be checked whose depiction is presented in fig. 10; the antisymmetrization of adjacent legs in the pentagon must give rise to a box numerator [36]. Given the special role played by the particle label one in the pure spinor representation described in section 4.2, the relations which involve its participation in a non-trivial way will be discussed separately.

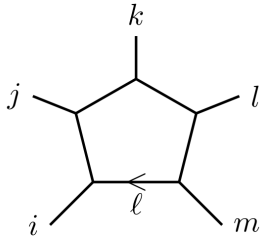

$N^{(5)}_{i|j,k,l,m}(\ell)$

Furthermore, the presence of the loop momentum in the pentagon numerator requires a precise convention for the mapping between a pentagon cubic graph and its pure spinor superspace representation: The loop momentum ℓ_m in the pentagon numerator must be chosen such that the four legs involved in the Jacobi identity have the same momentum in the three diagrams. Our convention is that for a given $N^{(5)}_{i|j,k,l,m}(\ell)$ labelling, ℓ is the momentum of the n-gon edge between the vertices with external legs i and m. For example, the kinematic Jacobi identity generated upon antisymmetrizing the legs 2 and 3 of the pentagon is given by

$$\langle N^{(4)}_{1|23,4,5}\rangle = \langle N^{(5)}_{1|2,3,4,5}(\ell) - N^{(5)}_{1|3,2,4,5}(\ell)\rangle\,, \tag{6.3}$$

and it is easily seen to be satisfied by their superspace representations for the pentagon given in (4.5). In (6.3), the expression for $N^{(5)}_{1|2,3,4,5}(\ell)$ is projected to the antisymmetric part with respect to legs 2 and 3 which amounts to $\frac{1}{2}V_1T_{23,4,5} - \frac{1}{2}V_1T_{32,4,5} = N^{(4)}_{1|23,4,5}$. The same argument applies to antisymmetrizations of $\langle N^{(5)}_{1|2,3,4,5}(\ell)\rangle$ in 3,4 or in 4,5.

When the Jacobi identity involves leg number one as seen in fig. 10 the analysis is a bit longer. Using the pentagon convention above, the second diagram in fig. 10 is written as[9] $N^{(5)}_{1|3,4,5,2}(\ell - k_2)$ and the kinematic Jacobi identity to verify is [37]

$$\langle N^{(4)}_{12|3,4,5}\rangle = \langle N^{(5)}_{1|2,3,4,5}(\ell) - N^{(5)}_{1|3,4,5,2}(\ell - k_2)\rangle. \tag{6.4}$$

Plugging in the explicit five-point box and pentagon numerators of (4.12) and (4.14) translates (6.4) into the following superspace statement[10]

$$\langle k_m^2 V_1 T^m_{2,3,4,5} + V_{21}T_{3,4,5} + V_1T_{23,4,5} + V_1T_{24,3,5} + V_1T_{25,3,4}\rangle = 0\,. \tag{6.5}$$

[9] This is equivalent to the "dihedral" symmetry condition of the pentagon numerator [36].

[10] That a external momentum contracted with the vector pentagon numerator gives rise to a sum of boxes like in (6.5) has already been derived in [37].

And indeed, one can show that (6.5) is BRST-trivial for five-point kinematics and therefore vanishes in the cohomology as computed by the pure spinor brackets $\langle\cdots\rangle$.

To see this recall that the superfield $D_{1|2|3,4,5}$ defined in equation (8.16) of [16],

$$D_{1|2|3,4,5} \equiv J_{2|1,3,4,5} + k_m^2 M^m_{12,3,4,5} + \big[s_{23} M_{123,4,5} + (3 \leftrightarrow 4,5)\big] \tag{6.6}$$

where $M^m_{12,3,4,5} = (1/s_{12}) T^m_{12,3,4,5}$ was shown to satisfy

$$QD_{1|2|3,4,5} = Y_{1,2,3,4,5} + k_m^2 C^m_{1|2,3,4,5} + \big[s_{23} C_{1|23,4,5} + (3 \leftrightarrow 4,5)\big]. \tag{6.7}$$

Using the expansion in (5.1) for the BRST invariants, $\langle QD_{1|2|3,4,5}\rangle = 0$ implies that

$$0 = \langle Y_{1,2,3,4,5} + k_m^2 V_1 T^m_{2,3,4,5} - \frac{s_{23}+s_{24}+s_{25}}{s_{12}} V_{21} T_{3,4,5} + V_1 T_{23,4,5} + V_1 T_{24,3,5} + V_1 T_{25,3,4}\rangle. \tag{6.8}$$

Since $\langle Y_{1,2,3,4,5}\rangle \propto \epsilon_{10} F^5$ vanishes by momentum conservation [26] and $s_{23}+s_{24}+s_{25} = -s_{12}$, the proof of (6.5) is complete. Therefore (4.2) furnishes a *local* BCJ-satisfying representation of the five-point one-loop SYM amplitude[11].

6.2. The five-point supergravity amplitude

Once a SYM amplitude has been presented in a form which satisfies all kinematic Jacobi identities $N_i(\ell) + N_j(\ell) + N_k(\ell) = 0$, it can be transformed into a gravity amplitude by trading color tensors for a second copy of the kinematic numerators, $c_i \to \tilde{N}_i(\ell)$ [3,28]. This allows to assemble the five-point supergravity amplitude at one-loop from the above box and pentagon numerators:

$$M_5 = \int \frac{d^D\ell}{(2\pi)^D} \sum_{\Gamma_i} \frac{\langle N_i(\ell)\tilde{N}_i(\ell)\rangle}{\prod_k P_{k,i}} \tag{6.9}$$

The combinatorics of the graph sum is explicit in the following representation

$$\begin{aligned} M_5 = \int \frac{d^D\ell}{(2\pi)^D} \Big\{ & \big[I^{(5)}_{1,2,3,4,5} N^{(5)}_{1|2,3,4,5}(\ell) \tilde{N}^{(5)}_{1|2,3,4,5}(\ell) + \text{symm}(2,3,4,5)\big] \\ & + \big[(I^{(4)}_{12,3,4,5} + \text{symm}(3,4,5)) N^{(4)}_{12|3,4,5} \tilde{N}^{(4)}_{12|3,4,5} + (2 \leftrightarrow 3,4,5)\big] \\ & + \big[(I^{(4)}_{1,23,4,5} + \text{symm}(23,4,5)) N^{(4)}_{1|23,4,5} \tilde{N}^{(4)}_{1|23,4,5} + (2,3|2,3,4,5)\big]\Big\} \end{aligned} \tag{6.10}$$

[11] One can also show that the manifestly BRST-invariant (and non-local) five-point representation of section 5.2 satisfies the BCJ duality conditions. Box numerators with particle one in the massive corner then vanish and the nonzero instances follow from permutations of $N^{(4)}_{1|23,4,5} = s_{23} C_{1|23,4,5}$ in $2,3,4,5$.

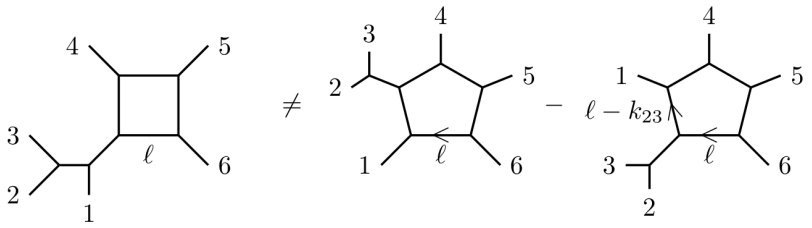

Fig. 11 Counterexample for kinematic Jacobi relations at six-points in the particular representation of section 4.4.

which can be confirmed by taking the field-theory limit[12] of the five-point closed-string amplitude in pure spinor superspace [29].

Depending on the relative chirality of the left- and right-moving superfields, the amplitude describes type IIA or type IIB supergravity. The tensor integrals in the pentagon numerators give rise to vector contractions between left- and right-moving superfields $\langle V_1 T^m_{2,3,4,5} \delta_{mn} \tilde{V}_1 \tilde{T}^n_{2,3,4,5} \rangle$. Components where both sides contribute through an ϵ_{10} tensor change signs between type IIA and type IIB and only the integrated type IIB amplitude can be written in terms of bilinears of SYM trees, see [29] for details.

6.3. The six-point amplitude and BCJ duality

In spite of many encouraging antisymmetrization properties of the six-point numerators, the BCJ duality is not satisfied by the local representation given in section 4.4. That is why we restrict the discussion to a counterexample. As depicted in fig. 11, the antisymmetrization of a massive pentagon numerator in external trees 1 and 23 is related to a one-mass box by the duality,

$$\langle N^{(4)}_{231|4,5,6} \rangle \leftrightarrow \langle N^{(5)}_{1|4,5,6,23}(\ell - k_{23}) - N^{(5)}_{1|23,4,5,6}(\ell) \rangle \ . \tag{6.11}$$

The left-hand side is given by $\langle V_{231} T_{4,5,6} \rangle$, and the right-hand side can be evaluated using the general pentagon numerators (4.14). The failure of (6.11) is then described by

$$\begin{aligned} &N^{(5)}_{1|23,4,5,6}(\ell) - N^{(5)}_{1|4,5,6,23}(\ell - k_{23}) + N^{(4)}_{231|4,5,6} \\ &\quad = k^{23}_m V_1 T^m_{23,4,5,6} + V_{231} T_{4,5,6} + \big[V_1 T_{234,5,6} + (4 \leftrightarrow 5,6) \big] \ . \end{aligned} \tag{6.12}$$

[12] The RNS derivation of the field-theory limit can be found in [38], the techniques are similar to the material of appendix A combined with the tensor integral (4.37).

However, since the right-hand side of (6.12) is not BRST closed it cannot be zero in the cohomology, therefore (6.11) cannot be an equality. In fact, one can show from $\langle QJ_{23|1,4,5,6}\rangle = 0$ that the pure spinor bracket of the right-hand side of (6.12) evaluates to

$$-\langle Y_{23,1,4,5,6}\rangle - s_{23}\langle V_2 J_{3|1,4,5,6} - V_3 J_{2|1,4,5,6}\rangle\,. \tag{6.13}$$

So the particular representation of the six-point amplitude obtained with the method of this paper does not satisfy the color-kinematics duality[13]. It will be interesting to check whether the derivation of local BCJ representations for n-point SYM tree amplitudes in [14] has an analogue at one-loop or whether the failure in (6.13) signals a subtle relation with the hexagon anomaly.

7. Conclusion

In this work, we have presented local representations for the one-loop integrand of five- and six-point SYM amplitudes in ten dimensions. Pure spinor superspace allows to express each numerator as a compact combination of superfields which were determined by BRST symmetry. Moreover, the multiparticle superfields $[A^B_\alpha, A^m_B, W^\alpha_B, F^{mn}_B]$ of [12] gave rise to a universal structure for box and pentagon numerators

$$\begin{aligned} N^{(4)}_{A|B,C,D} &\equiv V_A T_{B,C,D} \\ N^{(5)}_{A|B,C,D,E}(\ell) &\equiv \ell_m V_A T^m_{B,C,D,E} + \frac{1}{2}\big[V_{[A,B]}T_{C,D,E} + (B\leftrightarrow C,D,E)\big] \\ &\quad + \frac{1}{2}\big[V_A T_{[B,C],D,E} + (B,C|B,C,D,E)\big]\,, \end{aligned} \tag{7.1}$$

regardless of the external tree subdiagrams $A, B, \ldots, E$. As explained in [12], the bracketing notation merges two multiparticle slots such as to connect the associated cubic diagrams through a cubic vertex. Iterated bracketing is then expected to capture the structure of higher n-gon numerators, e.g. the hexagon numerator in section 4.4 should generalize as

$$\begin{aligned} N^{(6)}_{A|B,C,D,E,F}(\ell) &\equiv \frac{1}{2}\ell_m\ell_n V_A T^{mn}_{B,C,D,E,F} + \frac{1}{2}\ell_m V_{[A,B]}T^m_{C,D,E,F} + \frac{1}{2}\ell_m V_A T^m_{[B,C],D,E,F} \\ &\quad + \frac{1}{6}(V_{[[A,B],C]} + V_{[[C,B],A]})T_{D,E,F} + \frac{1}{6}V_A(T_{[[B,C],D],E,F} + T_{[[D,C],B],E,F}) \\ &\quad + \frac{1}{4}V_{[A,B]}T_{[C,D],E,F} + \frac{1}{4}V_A T_{[B,C],[D,E],F} - \frac{1}{12}(k^A_m - k^B_m)V_{[A,B]}T^m_{C,D,E,F} \\ &\quad - \frac{1}{12}(k^B_m - k^C_m)V_A T^m_{[B,C],D,E,F} - \frac{1}{24}V_A T^{mn}_{B,C,D,E,F}k^A_m k^A_n + \text{permutations}\,, \end{aligned} \tag{7.2}$$

[13] See [39,37] for four-dimensional BCJ representations of one-loop amplitudes.

where the sum of permutations follows the patterns of (4.33) and (4.35).

The ℓ-dependent parts of the above numerators exhibit a recursive structure and mimic the pattern of scalar lower-gon representatives upon adjusting the building blocks $T_{A,B,C} \to T^{m,\cdots}_{A,B,C,D,\cdots}$ to higher rank. Hence, the main leftover challenge in n-point amplitudes at higher multiplicity $n \geq 7$ is posed by the scalar part of the irreducible n-gon numerator which can be systematically addressed by demanding BRST invariance [32]. Minor redefinitions are required for massive corners subtending the first and last leg n and 1. The six-point example has been analyzed in section 4.4 and identified to play an essential role for the hexagon anomaly.

A manifestly BRST pseudo-invariant presentation of the amplitudes is given in section 5. Most of the integrals with leg one in a massive corner are eliminated which in turn assembles pseudo-invariant kinematic factors $C^{m,\cdots}_{1|\cdots}$ and $P_{1|6|2,3,4,5}$ classified in [16]. Their gluonic components can be downloaded from [19], and the scalars $C_{1|A,B,C}$ along with boxes can be expressed in terms of SYM tree [12].

The BCJ duality between color and kinematics is imprinted into the symmetries of multiparticle superfields [12] underlying V_A and $T^{m,\cdots}_{B,C,\cdots}$ and therefore respected by any tree subdiagram. However, this does not necessarily imply the kinematic Jacobi relations between numerators of p-gons and $(p-1)$-gons. At five points, the bracket structure of the pentagon numerator (7.1) and the identity (6.5) relating $k_m^2 V_1 T^m_{2,3,4,5}$ to box numerators guarantee that the representations of the integrand in both section 4.2 and 5.2 satisfy the duality. At six points, on the other hand, obstructions of the form $Y_{23,1,4,5,6}$ and $V_2 J_{3|1,4,5,6}$ in certain dual Jacobi relations might signal a subtle connection to the hexagon anomaly. It would be interesting to explore the physical meaning of this observation.

A valuable and complementary viewpoint on the SYM integrands of this work stems from the field-theory limit of the open superstring. The five-point case is discussed in appendix A based on the worldsheet integrand in [40], and string amplitudes at higher multiplicity provide a rich laboratory to study the interplay between the hexagon anomaly cancellation in string theory [25] and its appearance in field-theory [15].

Furthermore, it would be interesting to connect the BRST structures with other approaches to loop amplitudes such as ambitwistor strings [41]. Their pure spinor implementation [42] is know from [43] to reproduce the tree-level amplitudes following from BRST methods of [9].

Finally, the dictionary between cubic one-loop diagrams and superfields such as $V_A T_{B,C,D}$ suggest a generalization to higher loops. The two-loop analysis of [44] in the

minimal pure spinor formalism and the advances at three loops in [45] using its non-minimal version [46] furnish an encouraging starting point.

Acknowledgements: We thank Henrik Johansson for useful comments on the draft, Yu-tin Huang and Piotr Tourkine for helpful discussions and Michael Green for collaboration on related topics. OS is indebted to Song He for insightful discussions and collaboration on related topics. CRM and OS cordially thank the Institute of Advanced Study at Princeton for hospitality during early stages of this work. OS is grateful to the Department of Applied Mathematics and Theoretical Physics of the University of Cambridge for hospitality during completion of this work. CRM and OS acknowledge financial support by the European Research Council Advanced Grant No. 247252 of Michael Green. This work was supported in part by National Science Foundation Grant No. PHYS-1066293 and the hospitality of the Aspen Center for Physics.

Appendix A. The field-theory limit of the five-point superstring amplitude

In this appendix, we show that the five-point one-loop SYM amplitude presented in subsection 4.2 is reproduced by the field-theory limit of the open pure spinor superstring. This endeavour requires a matching of the Schwinger parametrization of Feynman integrals with the $\alpha' \to 0$ limit of the one-loop string amplitude prescription (3.5).

A.1. Schwinger parametrization of the five-point SYM amplitude

The string-based formalism for field-theory amplitudes [30] provides a convenient worldline representation of a scalar n-gon integral in D dimensions. The scalar box and pentagon integrals in the five-point amplitude can be written as the worldline integral

$$\int d^D\ell\, I^{(4)}_{12,3,4,5} = \pi^4 \int_0^\infty \frac{dt}{t}\, t^{4-D/2} \int\limits_{0\le\nu_i\le\nu_{i+1}\le 1} d\nu_2\, d\nu_3\, d\nu_4\, e^{-\pi t Q_4[k_{12},k_3,k_4,k_5]}\Big|_{\nu_1=0} \tag{A.1}$$

$$\int d^D\ell\, I^{(5)}_{1,2,3,4,5} = \pi^5 \int_0^\infty \frac{dt}{t}\, t^{5-D/2} \int\limits_{0\le\nu_i\le\nu_{i+1}\le 1} d\nu_2\, d\nu_3\, d\nu_4\, d\nu_5\, e^{-\pi t Q_5[k_1,k_2,k_3,k_4,k_5]}\Big|_{\nu_1=0} \tag{A.2}$$

with exponents

$$Q_n[k_{A_1}, k_{A_2}, \ldots, k_{A_n}] \equiv \sum_{i<j}^{n} (k_{A_i}\cdot k_{A_j})(\nu_{ij}^2 - |\nu_{ij}|) \tag{A.3}$$

and shorthand notation $\nu_{ij} \equiv \nu_i - \nu_j$. The transformation from momentum space to the worldline picture involves a Gaussian integration over the shifted loop momentum $\hat{\ell}^m \equiv \ell^m + \sum_{i=1}^n k_{A_i}^m \nu_i$. Hence, vector integrals follow from substituting $\ell^m \to -\sum_{i=1}^n k_{A_i}^m \nu_i$, e.g.

$$\int d^D\ell\, I^{(5)}_{1,2,3,4,5}\, \ell^m = -\pi^5 \int_0^\infty \frac{dt}{t}\, t^{5-D/2} \int\limits_{0\le\nu_i\le\nu_{i+1}\le 1} d\nu_2\, \ldots\, d\nu_5 \sum_{i=1}^5 k_i^m \nu_i\, e^{-\pi t Q_5[k_1,\ldots,k_5]}\ . \quad \text{(A.4)}$$

In the pentagon contribution (4.4) and (4.5) to the five-point SYM amplitude, scalar and vector parts can be cast into a unified form using the cohomology manipulations [29,16]

$$\begin{aligned} \langle V_1 k_m^1 T^m_{2,3,4,5}\rangle &= \langle -V_{12}T_{3,4,5} + (2\leftrightarrow 3,4,5)\rangle \\ \langle V_1 k_m^2 T^m_{2,3,4,5}\rangle &= \langle V_{12}T_{3,4,5} + \big[-V_1 T_{23,4,5} + (3\leftrightarrow 4,5)\big]\rangle \end{aligned} \quad \text{(A.5)}$$

to express $\sum_{i=1}^5 \nu_i k_m^i \langle V_1 T^m_{2,3,4,5}\rangle$ in terms of box numerators. The pentagon integrals (A.2) and (A.4) then conspire to

$$\begin{aligned} \int d^D\ell\, \langle A_{\rm pent}(1,2,3,4,5|\ell)\rangle &= \pi^4 \int_0^\infty \frac{dt}{t}\, t^{5-D/2} \int\limits_{0\le\nu_i\le\nu_{i+1}\le 1} d\nu_2\, \ldots\, d\nu_5\, e^{-\pi t Q_5[k_1,k_2,\ldots,k_5]} \\ &\times \Big\langle \big[\partial_\nu G_{12} V_{12} T_{3,4,5} + (2\leftrightarrow 3,4,5)\big] + V_1\big[\partial_\nu G_{23} T_{23,4,5} + (2,3|2,3,4,5)\big]\Big\rangle \end{aligned} \quad \text{(A.6)}$$

with the derivative of the worldline Green function

$$G_{ij} \equiv \frac{\pi}{2}\big(\nu_{ij}^2 - |\nu_{ij}|\big)\ , \qquad \partial_\nu G_{ij} \equiv \pi\Big(\nu_{ij} - \frac{1}{2}{\rm sgn}(\nu_{ij})\Big)\ . \quad \text{(A.7)}$$

This is a convenient starting point to make contact with the corresponding superstring amplitude. The sign function in (A.7) is defined to be $+1$ (-1) when $\nu_i \ge \nu_j$ $(\nu_i < \nu_j)$.

For the box contribution (4.3) to the five-point amplitude, the Schwinger parametrization directly follows from (A.1) and minor cyclic modifications

$$\begin{aligned} \int d^D\ell\, \langle A_{\rm box}(1,2,3,4,5)\rangle = \pi^4 \int_0^\infty \frac{dt}{t}\, t^{4-D/2} \int\limits_{0\le\nu_i\le\nu_{i+1}\le 1} d\nu_2\, d\nu_3\, d\nu_4 \Big\{ &\langle V_{12}T_{3,4,5}\rangle e^{-\pi t Q_4[k_{12},k_3,k_4,k_5]} \\ &+ \langle V_1 T_{23,4,5}\rangle e^{-\pi t Q_4[k_1,k_{23},k_4,k_5]} + \langle V_1 T_{2,34,5}\rangle e^{-\pi t Q_4[k_1,k_2,k_{34},k_5]} \\ &+ \langle V_1 T_{2,3,45}\rangle e^{-\pi t Q_4[k_1,k_2,k_3,k_{45}]} + \langle V_{51} T_{2,3,4}\rangle e^{-\pi t Q_4[k_{51},k_2,k_3,k_4]} \Big\}\Big|_{\nu_1=0}\ . \end{aligned} \quad \text{(A.8)}$$

Note that the exponents Q_4 as in (A.3) associated with boxes arise from degenerations of the pentagon, e.g. $Q_4[k_1,k_{23},k_4,k_5] = Q_5[k_1,k_2,\ldots,k_5]\big|_{\nu_2=\nu_3}$.

A.2. Worldline limit of open string one-loop amplitudes

As described in [22], the field-theory limit of the superstring is obtained by setting $\alpha' \to 0$ and by degenerating the genus-one surface with modular parameter $\mathrm{Im}(\tau) \to \infty$. These are the limits in which strings shrink to point-particles, and the worldsheet surface reduces to point-particle worldline diagrams. Moreover, these limits must be performed such that the proper time $t \equiv \alpha' \,\mathrm{Im}(\tau)$ and the worldsheet positions $z_j \equiv \mathrm{Re}(z_j) + i\,\mathrm{Im}(\tau)\nu_j$ stay finite. In this limit, the worldsheet Green function

$$\mathcal{G}_{ij} \equiv -\frac{\alpha'}{2}\Big(\ln\big|\theta_1(z_{ij}|\tau)\big| - \pi\frac{\mathrm{Im}(z_{ij})^2}{\mathrm{Im}(\tau)}\Big) \tag{A.9}$$

loses its dependence on the real part of $z_{ij} \equiv z_i - z_j$ and reproduces the Green function (A.7) of the worldline upon identifying $\mathrm{Im}(z_j) = t\nu_j$ with the worldline insertion points ν_j,

$$\mathcal{G}_{ij} \to t\, G_{ij} \ , \qquad \partial_z \mathcal{G}_{ij} \to \partial_\nu G_{ij} \ . \tag{A.10}$$

A key ingredient of the worldsheet correlator in the string amplitude (3.5) is the ubiquitous Koba–Nielsen factor which reduces as follows under the field-theory limit (A.10):

$$\mathcal{I} \equiv \Big\langle \prod_{j=1}^n e^{ik_j\cdot x(z_j,\overline{z}_j)} \Big\rangle = \frac{1}{(\mathrm{Im}\ \tau)^5}\prod_{j<k} e^{-2s_{jk}\mathcal{G}_{jk}} \to \frac{1}{t^5} e^{-\pi t Q_n[k_1,k_2,\ldots,k_n]} \ . \tag{A.11}$$

The plane waves from the vertex operators reproduce the exponential (A.3) of the Feynman integrals' worldline parametrization in (A.2) and (4.37). Similarly, the worldline integration over t and ν_i descends from the worldsheet integration in (3.5) over the cylinder boundary,

$$\int_0^\infty \frac{dt}{t^5} \int\limits_{0\leq \mathrm{Im}\, z_i \leq \mathrm{Im}\, z_{i+1}\leq t} dz_2\, dz_3\, \ldots\, dz_n \to \int_0^\infty \frac{dt}{t}\, t^{n-D/2} \int\limits_{0\leq \nu_i\leq \nu_{i+1}\leq 1} d\nu_2\, d\nu_3\, \ldots\, d\nu_n \ . \tag{A.12}$$

However, before the combined limit of $\alpha' \to 0$ and $\mathrm{Im}(\tau) \to \infty$ can be performed in (A.11), an additional feature of the Koba–Nielsen factor has to be taken into account which is completely absent in its worldline counterpart $e^{-\pi t Q_N}$: It is the source of kinematic poles when the vertex operator positions $z_i \to z_j$ approach each other.

More precisely, the short-distance behaviour of (A.11) as $z_i \to z_j$ is governed by $\mathcal{I} \sim |z_{ij}|^{\alpha' k_i\cdot k_j}$. Additional factors of worldsheet propagators $\partial_z \mathcal{G}_{ij} \to z_{ij}^{-1} + \mathcal{O}(z_{ij})$ modify the leading singular behavior to $\mathcal{I}\partial_z\mathcal{G}_{ij} \sim |z_{ij}|^{\alpha' k_i\cdot k_j - 1}$. In this case, the integration domain where $|z_{ij}| \ll 1$ gives rise to a pole in $\alpha' k_i\cdot k_j$ with $z_i = z_j$ on its residue[14]. In other words, if i and j are adjacent on the worldsheet boundary, the following kinematic pole emerges:

$$\mathcal{I}\,\partial_z \mathcal{G}_{i,i+1} \to \mathcal{I}\,\frac{\delta(z_i - z_{i+1})}{s_{i,i+1}} \ + \ \mathcal{O}(s^0_{i,i+1}) \ . \tag{A.13}$$

This mechanism is the origin of box integrals in the five-point open string amplitude.

[14] This can be understood from the delta function representation $\delta(x) = \lim_{s\to 0} s x^{s-1}$.

A.3. Worldline limit of the five-point open string amplitude

The above procedure to perform the point particle limit is now applied to the pure spinor prescription for the five-point open superstring amplitude in (3.5). The constraints from zero-mode saturation [23] allow for one OPE among the vertex operators. Hence, the correlator[15] follows from summing over the ten BRST blocks capturing the OPE contractions [40],

$$\begin{aligned}&\langle b\,\mathcal{Z}\,V^1(z_1)\,U^2(z_2)\,\ldots\,U^5(z_5)\rangle = \mathcal{I}\cdot\mathcal{K}_5\\ &\mathcal{K}_5 \equiv \Big\langle \big[\partial_z\mathcal{G}_{12}V_{12}T_{3,4,5} + (2\leftrightarrow 3,4,5)\big] + \big[\partial_z\mathcal{G}_{23}V_1T_{23,4,5} + (2,3|2,3,4,5)\big]\Big\rangle\ . \end{aligned} \tag{A.14}$$

The kinematic factor $\mathcal{K}_5$ is the generating function for the numerators of both the boxes and the pentagon. According to (A.11) and (A.12), the worldline limit reduces the plane wave correlator and the worldsheet integrations in the string amplitude to the Schwinger parametrization of the pentagon:

$$\mathcal{A}_5^{\rm pent} \to \int_0^\infty \frac{dt}{t}\, t^{5-D/2} \int\limits_{0\le\nu_i\le\nu_{i+1}\le 1} d\nu_2\,\ldots\,d\nu_5\, e^{-\pi t Q_5[k_1,k_2,\ldots,k_5]}\,\big(\mathcal{K}_5\,\big|_{\partial_z\mathcal{G}_{ij}\to\partial_z G_{ij}}\big)\ . \tag{A.15}$$

The worldline limit of the Green functions (A.10) directly maps the open string kinematic factor $\mathcal{K}_5$ to the Schwinger integrand (A.6) of the pentagon numerator $N^{(5)}_{1|2,3,4,5}$, hence

$$\mathcal{A}_5^{\rm pent} \to \int d^D\ell\,\langle A_{\rm pent}(1,2,3,4,5|\ell)\rangle\ . \tag{A.16}$$

In addition, boxes arise from the singular limit (A.13) when the positions z_i, z_{i+1} of neighboring vertex operators collide. This applies to the cyclic orbit of the propagator $\partial_z\mathcal{G}_{12}$ which leaves $\delta(z_1-z_2)$ at the residue of the pole in s_{12}:

$$\begin{aligned}\mathcal{A}_5^{\rm box} = \int_0^\infty dt \int\limits_{0\le{\rm Im}\,z_i\le{\rm Im}\,z_{i+1}\le t} \mathcal{I}\,\Big\langle &\frac{\delta(z_{12})}{s_{12}}V_{12}T_{3,4,5} + \frac{\delta(z_{23})}{s_{23}}V_1T_{23,4,5}\\ &+\frac{\delta(z_{34})}{s_{34}}V_1T_{2,34,5} + \frac{\delta(z_{45})}{s_{45}}V_1T_{2,3,45} + \frac{\delta(z_{51})}{s_{15}}V_{51}T_{2,3,4}\Big\rangle\ .\end{aligned} \tag{A.17}$$

The same worldline limits (A.11) and (A.12) applied to the irreducible part of the correlator reduce (A.17) to the Schwinger parametrization of the boxes in (A.8),

$$\mathcal{A}_5^{\rm box} \to \int d^D\ell\,\langle A_{\rm box}(1,2,3,4,5)\rangle\ , \tag{A.18}$$

[15] See for instance [47] for the analogous RNS computation which reproduces the bosonic components of (A.14) up to total derivatives.

using $\delta(z_1 - z_2) \sim t^{-1}\delta(\nu_1 - \nu_2)$ and $Q_4[k_{12}, k_3, k_4, k_5] = Q_5[k_1, k_2, \ldots, k_5]\big|_{\nu_1=\nu_2}$.

To summarize, the point-particle limit of the five-point open string amplitude (3.5) contains a reducible part caused by the singular behavior (A.13) which reproduces the boxes of our superspace proposal, see (A.18). For the irreducible part, on the other hand, the degeneration limit of the Green function (A.10) is applied directly to $\mathcal{K}_5$ and reproduces the pentagon numerator (4.5) found by the BRST analysis, see (A.18).

An analogous analysis can be carried out for the manifestly BRST invariant form of the string amplitude [40],

$$\mathcal{A}_5 = \int_0^\infty dt \int\limits_{0\leq \mathrm{Im}\, z_i \leq \mathrm{Im}\, z_{i+1}\leq t} \mathcal{I}\, \langle s_{23}\partial_z \mathcal{G}_{23}\, C_{1|23,4,5} + (2,3|2,3,4,5)\rangle \ , \tag{A.19}$$

related to $\mathcal{K}_5$ in (A.14) by integration by parts with respect to $z_2, \ldots, z_5$. Using the same distinction between box and pentagon contributions as above, (A.19) reduces to the manifestly BRST invariant representation (5.5) of the field-theory limit. The Schwinger parametrization of the scalar and vector pentagons can be coherently described by ∂G_{ij} once the following cohomology manipulations are taken into account [16]

$$\langle k^1_m C^m_{1|2,3,4,5}\rangle = 0 \ , \quad \langle k^2_m C^m_{1|2,3,4,5}\rangle = -\langle s_{23} C_{1|23,4,5} + (3 \leftrightarrow 4,5)\rangle \ . \tag{A.20}$$

Note that they follow from (6.5) under the prescription (5.4) to manifest BRST invariance.

References

[1] H. Elvang and Y. t. Huang, "Scattering Amplitudes," [arXiv:1308.1697 [hep-th]].

[2] L. Brink, J. H. Schwarz and J. Scherk, "Supersymmetric Yang-Mills Theories," Nucl. Phys. B **121**, 77 (1977)..

[3] Z. Bern, J.J.M. Carrasco and H. Johansson, "New Relations for Gauge-Theory Amplitudes," Phys. Rev. D **78**, 085011 (2008). [arXiv:0805.3993 [hep-ph]].

[4] N. Berkovits, "ICTP lectures on covariant quantization of the superstring," [hep-th/0209059].

[5] O.A. Bedoya and N. Berkovits, "GGI Lectures on the Pure Spinor Formalism of the Superstring," [arXiv:0910.2254 [hep-th]].

[6] N. Berkovits, "Twistor Origin of the Superstring," [arXiv:1409.2510 [hep-th]].

[7] N. Berkovits, "Super-Poincare covariant quantization of the superstring," JHEP **0004**, 018 (2000) [arXiv:hep-th/0001035].

[8] P.S. Howe, "Pure Spinors Lines In Superspace And Ten-Dimensional Supersymmetric Theories," Phys. Lett. B **258**, 141 (1991) [Addendum-ibid. B **259**, 511 (1991)]. ;
P.S. Howe, "Pure Spinors, Function Superspaces And Supergravity Theories In Ten-Dimensions And Eleven-Dimensions," Phys. Lett. B **273**, 90 (1991).

[9] C.R. Mafra, O. Schlotterer, S. Stieberger and D. Tsimpis, "A recursive method for SYM n-point tree amplitudes," Phys. Rev. D **83**, 126012 (2011). [arXiv:1012.3981 [hep-th]].

[10] C.R. Mafra, O. Schlotterer and S. Stieberger, "Complete N-Point Superstring Disk Amplitude I. Pure Spinor Computation," Nucl. Phys. B **873**, 419 (2013). [arXiv:1106.2645 [hep-th]]. ;
C.R. Mafra, O. Schlotterer and S. Stieberger, "Complete N-Point Superstring Disk Amplitude II. Amplitude and Hypergeometric Function Structure," Nucl. Phys. B **873**, 461 (2013). [arXiv:1106.2646 [hep-th]].

[11] E.Witten, "Twistor-Like Transform In Ten-Dimensions" Nucl.Phys. B **266**, 245 (1986)

[12] C.R. Mafra and O. Schlotterer, "Multiparticle SYM equations of motion and pure spinor BRST blocks," JHEP **1407**, 153 (2014). [arXiv:1404.4986 [hep-th]].

[13] C.R. Mafra, "Towards Field Theory Amplitudes From the Cohomology of Pure Spinor Superspace," JHEP **1011**, 096 (2010). [arXiv:1007.3639 [hep-th]].

[14] C.R. Mafra, O. Schlotterer and S. Stieberger, "Explicit BCJ Numerators from Pure Spinors," JHEP **1107**, 092 (2011). [arXiv:1104.5224 [hep-th]].

[15] P. H. Frampton and T. W. Kephart, "Explicit Evaluation of Anomalies in Higher Dimensions," Phys. Rev. Lett. **50**, 1343 (1983), [Erratum-ibid. **51**, 232 (1983)]. ;
P. H. Frampton and T. W. Kephart, "The Analysis of Anomalies in Higher Space-time Dimensions," Phys. Rev. D **28**, 1010 (1983).

[16] C.R. Mafra and O. Schlotterer, "Cohomology foundations of one-loop amplitudes in pure spinor superspace," [arXiv:1408.3605 [hep-th]].

[17] J.P. Harnad and S. Shnider, "Constraints And Field Equations For Ten-Dimensional Superyang-Mills Theory," Commun. Math. Phys. **106**, 183 (1986) ;
P.A. Grassi and L. Tamassia, "Vertex operators for closed superstrings," JHEP **0407**, 071 (2004) [arXiv:hep-th/0405072]. ;
G. Policastro and D. Tsimpis, "R^4, purified," Class. Quant. Grav. **23**, 4753 (2006) [arXiv:hep-th/0603165].

[18] C.R. Mafra, "PSS: A FORM Program to Evaluate Pure Spinor Superspace Expressions," [arXiv:1007.4999 [hep-th]]. ;
J.A.M. Vermaseren, "New features of FORM," arXiv:math-ph/0010025. ;
M. Tentyukov and J.A.M. Vermaseren, "The multithreaded version of FORM," arXiv:hep-ph/0702279.

[19] C.R. Mafra and O. Schlotterer, `http://www.damtp.cam.ac.uk/user/crm66/SYM/pss.html`

[20] W. Siegel, "Classical Superstring Mechanics," Nucl. Phys. **B263**, 93 (1986).

[21] C.R. Mafra, "Pure Spinor Superspace Identities for Massless Four-point Kinematic Factors," JHEP **0804**, 093 (2008). [arXiv:0801.0580 [hep-th]]. ;
C.R. Mafra, "Simplifying the Tree-level Superstring Massless Five-point Amplitude," JHEP **1001**, 007 (2010). [arXiv:0909.5206 [hep-th]]. ;
C.R. Mafra, O. Schlotterer, S. Stieberger and D. Tsimpis, "Six Open String Disk Amplitude in Pure Spinor Superspace," Nucl. Phys. B **846**, 359 (2011). [arXiv:1011.0994 [hep-th]].

[22] M. B. Green, J. H. Schwarz and L. Brink, "N=4 Yang-Mills and N=8 Supergravity as Limits of String Theories," Nucl. Phys. B **198**, 474 (1982).

[23] N. Berkovits, "Multiloop amplitudes and vanishing theorems using the pure spinor formalism for the superstring," JHEP **0409**, 047 (2004). [hep-th/0406055].

[24] M.B. Green, J.H. Schwarz and E. Witten, "Superstring Theory. Vol. 2: Loop Amplitudes, Anomalies And Phenomenology," Cambridge, UK: Univ. Pr. (1987) 596 P. (Cambridge Monographs On Mathematical Physics).

[25] M. B. Green and J. H. Schwarz, "Anomaly Cancellation in Supersymmetric D=10 Gauge Theory and Superstring Theory," Phys. Lett. B **149**, 117 (1984). ;
M.B. Green and J.H. Schwarz, "The Hexagon Gauge Anomaly in Type I Superstring Theory," Nucl. Phys. B **255**, 93 (1985).

[26] N. Berkovits and C.R. Mafra, "Some Superstring Amplitude Computations with the Non-Minimal Pure Spinor Formalism," JHEP **0611**, 079 (2006). [hep-th/0607187].

[27] Z. Bern, L. J. Dixon, D. C. Dunbar and D. A. Kosower, "One loop n point gauge theory amplitudes, unitarity and collinear limits," Nucl. Phys. B **425**, 217 (1994). [hep-ph/9403226].

[28] Z. Bern, J. J. M. Carrasco and H. Johansson, "Perturbative Quantum Gravity as a Double Copy of Gauge Theory," Phys. Rev. Lett. **105**, 061602 (2010). [arXiv:1004.0476 [hep-th]].

[29] M.B. Green, C.R. Mafra and O. Schlotterer, "Multiparticle one-loop amplitudes and S-duality in closed superstring theory," JHEP **1310**, 188 (2013). [arXiv:1307.3534].

[30] Z. Bern and D. A. Kosower, "Efficient calculation of one loop QCD amplitudes," Phys. Rev. Lett. **66**, 1669 (1991).. ;
Z. Bern and D. A. Kosower, "The Computation of loop amplitudes in gauge theories," Nucl. Phys. B **379**, 451 (1992).. ;
M. J. Strassler, "Field theory without Feynman diagrams: One loop effective actions," Nucl. Phys. B **385**, 145 (1992). [hep-ph/9205205]. ;
Z. Bern, D. C. Dunbar and T. Shimada, "String based methods in perturbative gravity," Phys. Lett. B **312**, 277 (1993). [hep-th/9307001]. ;
D. C. Dunbar and P. S. Norridge, "Calculation of graviton scattering amplitudes using string based methods," Nucl. Phys. B **433**, 181 (1995). [hep-th/9408014]. ;
C. Schubert, "Perturbative quantum field theory in the string inspired formalism," Phys. Rept. **355**, 73 (2001). [hep-th/0101036]. ;
N. E. J. Bjerrum-Bohr and P. Vanhove, "Absence of Triangles in Maximal Supergravity Amplitudes," JHEP **0810**, 006 (2008). [arXiv:0805.3682 [hep-th]].

[31] W.M. Chen, Y. t. Huang and D. A. McGady, "Anomalies without an action," [arXiv:1402.7062 [hep-th]].

[32] C.R. Mafra and O. Schlotterer, work in progress

[33] Z. Bern, J. J. M. Carrasco, L. J. Dixon, H. Johansson and R. Roiban, "Simplifying Multiloop Integrands and Ultraviolet Divergences of Gauge Theory and Gravity Amplitudes," Phys. Rev. D **85**, 105014 (2012). [arXiv:1201.5366 [hep-th]]. ;
Z. Bern, S. Davies, T. Dennen, A. V. Smirnov and V. A. Smirnov, "Ultraviolet Properties of N=4 Supergravity at Four Loops," Phys. Rev. Lett. **111**, no. 23, 231302 (2013). [arXiv:1309.2498 [hep-th]]. ;
Z. Bern, S. Davies and T. Dennen, "Enhanced Ultraviolet Cancellations in N = 5 Supergravity at Four Loop," [arXiv:1409.3089 [hep-th]].

[34] A. Ochirov and P. Tourkine, "BCJ duality and double copy in the closed string sector," JHEP **1405**, 136 (2014). [arXiv:1312.1326 [hep-th]].

[35] Z. Bern, S. Davies, T. Dennen, Y. t. Huang and J. Nohle, "Color-Kinematics Duality for Pure Yang-Mills and Gravity at One and Two Loops," [arXiv:1303.6605 [hep-th]].

[36] J.J. Carrasco and H. Johansson, "Five-Point Amplitudes in N=4 Super-Yang-Mills Theory and N=8 Supergravity," Phys. Rev. D **85**, 025006 (2012). [arXiv:1106.4711 [hep-th]].

[37] N.E.J. Bjerrum-Bohr, T. Dennen, R. Monteiro and D. O'Connell, "Integrand Oxidation and One-Loop Colour-Dual Numerators in N=4 Gauge Theory," JHEP **1307**, 092 (2013). [arXiv:1303.2913 [hep-th]].

[38] N.E.J. Bjerrum-Bohr and P. Vanhove, "Explicit Cancellation of Triangles in One-loop Gravity Amplitudes," JHEP **0804**, 065 (2008). [arXiv:0802.0868 [hep-th]].

[39] E. Y. Yuan, "Virtual Color-Kinematics Duality: 6-pt 1-Loop MHV Amplitudes," JHEP **1305**, 070 (2013). [arXiv:1210.1816 [hep-th]].

[40] C.R. Mafra and O. Schlotterer, "The Structure of n-Point One-Loop Open Superstring Amplitudes," JHEP **1408**, 099 (2014). [arXiv:1203.6215 [hep-th]].

[41] L. Mason and D. Skinner, "Ambitwistor strings and the scattering equations," JHEP **1407**, 048 (2014). [arXiv:1311.2564 [hep-th]]. ;
T. Adamo, E. Casali and D. Skinner, "Ambitwistor strings and the scattering equations at one loop," JHEP **1404**, 104 (2014). [arXiv:1312.3828 [hep-th]].

[42] N. Berkovits, "Infinite Tension Limit of the Pure Spinor Superstring," JHEP **1403**, 017 (2014). [arXiv:1311.4156 [hep-th], arXiv:1311.4156].

[43] H. Gomez and E. Y. Yuan, "N-point tree-level scattering amplitude in the new Berkovits' string," JHEP **1404**, 046 (2014). [arXiv:1312.5485 [hep-th]].

[44] N. Berkovits, "Super-Poincare covariant two-loop superstring amplitudes," JHEP **0601**, 005 (2006). [hep-th/0503197].

[45] H. Gomez and C.R. Mafra, "The closed-string 3-loop amplitude and S-duality," JHEP **1310**, 217 (2013). [arXiv:1308.6567 [hep-th]].

[46] N. Berkovits, "Pure spinor formalism as an N=2 topological string," JHEP **0510**, 089 (2005). [hep-th/0509120].

[47] A. Tsuchiya, "More on One Loop Massless Amplitudes of Superstring Theories," Phys. Rev. D **39**, 1626 (1989).